https://doi.org/10.5194/essd-2021-55
Preprint. Discussion started: 3 March 2021

Open Access Earth System Science Data Discussions

UV-Indien Network ground-based measurements : comparisons with satellite and model estimates of UV radiation over the Western Indian Ocean.

Kevin Lamy[1], Thierry Portafaix[1], Colette Brogniez[2], Kaisa Lakkala[3,4], Mikko R.A. Pitkänen[4], Antti Arola[4], Jean-Baptiste Forestier[1], Vincent Amelie[5], Mohamed Abdoulwahab Toihir[6], and Solofoarisoa Rakotoniaina[7]

[1]LACy, Laboratoire de l'Atmosphère et des Cyclones (UMR 8105 CNRS, Université de La Réunion, Météo-France), Saint-Denis de La Réunion, France
[2]LOA, Laboratoire d'Optique Atmosphérique (Univ. Lille, CNRS - UMR 8518) Lille, France
[3]Space and Earth Observation Centre, Finnish Meteorological Institute, Sodankylä, Finland
[4]Climate Research Programme, Finnish Meteorological Institute, Kuopio, Finland
[5]Seychelles Meteorological Authority, Mahé, Seychelles
[6]Agence Nationale de l'Aviation Civile et de la Météorologie, Moroni, Comores
[7]IOGA, Institute and Observatory of Geophysics of Antananarivo (IOGA) University of Antananarivo, Madagascar

Correspondence: K. Lamy (kevin.lamy@univ-reunion.fr)

Abstract. As part of the UV-Indien Network, 9 ground-based stations have been equipped with one spectroradiometer, radiometers and all-sky cameras. These stations are homogeneously distributed in 5 countries of the Western Indian Ocean region (Comoros, France, Madagascar, Mauritius and Seychelles), a part of the world where almost no measurements have been made so far. The main scientific objectives of this network are to study the annual and inter-annual variability of the ultraviolet (UV) radiation in this area, to validate the output of numerical models and satellite estimates of ground-based UV measurements, and to monitor UV radiation in the context of climate change and projected ozone depletion in this region. The first results are presented here for the oldest stations (Antananarivo, Anse Quitor, Mahé and Saint-Denis). Ground-based measurements of UV index (UVI) are compared against satellite estimates (Ozone Monitoring Instrument (OMI), the TROPOspheric Monitoring Instrument (TROPOMI), the Global Ozone Monitoring Experiment (GOME) and model forecasts of UVI (Tropospheric Emission Monitoring Internet Service (TEMIS) and Copernicus Atmospheric Monitoring Service (CAMS). The median relative differences between satellite or model estimates and ground-based measurements of clear-sky UVI range between – 34.5 % and 15.8 %. Under clear skies, the smallest UVI median difference between the satellites or model estimates and the measurements of ground-based instruments is found to be 0.02 (TROPOMI), 0.04 (OMI), -0.1 (CAMS) and -0.4 (CAMS) at St-Denis, Antananarivo, Anse Quitor and Mahé respectively. The cloud fraction and UVI diurnal profile are calculated for these four stations. The mean UVI values at local solar noon range between 10 (Antananarivo, Anse Quitor and Saint-Denis) and 14 at Mahé. The mean UVIs in clear-sky conditions are higher than mean UVI in all-sky conditions, although it can still be noted that UVI maxima are higher for all-sky conditions than for clear sky conditions. This is the result of UVI enhancement induced by clouds, observed at these four stations. The greatest increase in UV radiation under cloudy conditions was observed at the

https://doi.org/10.5194/essd-2021-55
Preprint. Discussion started: 3 March 2021

Open Access Earth System Science Data Discussions

Mahé station, with increases of more than 4. The data used in this study is available at https://doi.org/10.5281/zenodo.4572026 (Lamy and Portafaix, 2021).

1 Introduction

Solar radiation produces a broad spectrum of radiation, in which wavelengths between 100 and 400 nm correspond to ultraviolet radiation (UVR). The UVR that reaches the Earth's surface has a direct effect on human health, terrestrial and aquatic ecosystems, and on the degradation of material (Bernhard et al., 2020).

UV has important effects on human health. These effects can be beneficial or harmful. For example, human exposure to UV-B ensures the synthesis of vitamin D, which is essential for bone mineralization. UVR is also known to be a powerful virus killer, which can explain some epidemiological pattern (Duan et al., 2003). On the other hand, UV-B can have a harmful effect by altering the DNA of cells. For humans, an increase in UV-B radiation increases the risk of skin cancer and the occurrence of cataracts and weakens the immune system.

The UV Index (UVI) was defined by the World Health Organization (WHO, 1995) to measure the amount of sunburn-producing UV radiation that reaches the surface. If the UVI is above 3, protection is necessary and, above 8, prolonged exposure can become dangerous. Indices above 11 are considered extreme.

Naturally, the geographical area corresponding to the tropics of the southern hemisphere (tropical and ocean-dominated environment) exposes populations to high levels of UV radiation. This is because the zenith angles of the sun are very small close to noon all year round and the amounts of stratospheric ozone or atmospheric aerosols are lower than at higher latitudes in continental regions. This is the case in most of the southern Indian Ocean (La Réunion, Madagascar, Mauritius, Seychelles, Comoros). UV indices in these regions can exceed 10 almost all year round, which implies serious consequences for the health of the populations. For example, dermatologists in Reunion Island (21°S, 55.5 °E) have noted a rapid increase in sun-induced skin lesions (Observatoire Régional de la Santé de La Réunion, 2008). The number of these lesions triples every 10 years, with an accelerating progression and affects more than 2% of the population. Radiation doses received by particularly exposed populations (children and outdoor workers) exceed dangerous thresholds in this region of the Indian Ocean almost all year round (Wright et al., 2013). Finally, it can be noted that all skin phototypes are concerned, including photo-types 5 and 6 (Sitek et al., 2016). An important part of this observed increase can be explained by lifestyle changes, and expansion in seaside activities and a constant increase in exposure to the sun. The development of tourism, especially local tourism, is a determining factor.

When UV radiation penetrates the atmosphere, its intensity along the atmospheric path and on the ground depends on various parameters, including geometric or geographical factors such as the solar zenith angle (SZA), latitude and altitude. Cloud cover plays an important role, generally reducing the intensity of radiation although under certain conditions, cloud cover can also increase the intensity, as it is the case of fractional cloud cover (Sabburg and Wong, 2000). Aerosols, small particles of natural (marine aerosols, volcanoes) or anthropogenic (biomass fires, fossil fuel combustion) origin, scatter and absorb UV radiation. If present in large quantities, they can strongly affect surface UV radiation or radiative forcing. The reflectivity of a surface, or

https://doi.org/10.5194/essd-2021-55
Preprint. Discussion started: 3 March 2021

Open Access Earth System Science Data Discussions

albedo, is also involved in modulating the intensity of radiation and, finally, the concentrations of certain gases, such as ozone, in the atmosphere plays an essential role. The amount of ozone (O_3) in the stratosphere largely drives UV levels on the ground because of ozone has a high absorption capacity in the UV wavelengths. O_3 is produced in the tropics under the influence of strong solar radiation and is transported towards the poles by the Brewer-Dobson circulation (BDC).

Ozone concentrations have been significantly depleted over the past 35 years due to emissions of halocarbons, which are both powerful greenhouse gases (GHGs) and ozone-depleting substances (ODS). The Montreal Protocol (1987) and its amendments are an undisputed success of environmental policy making and have slowly brought ODS amounts down almost to historical levels (Chipperfield et al., 2015).

However, the evolution of stratospheric ozone beyond the middle of the 21st century, when ODS emissions will be minimal and their atmospheric concentrations will continue to decrease, will be largely determined by the concentrations of certain greenhouse gases (GHGs) such as CO_2, N_2O and CH_4 (Eyring et al., 2013). On the other hand, the increase in CO_2 is expected to accelerate the BDC (Butchart, 2014; WMO, 2018). Ozone will then be transported more rapidly from the tropics to the poles and thus the total ozone column (TOC) will increase in mid-latitudes and decrease in the tropics. Since UV radiation at the surface is directly dependent on the total ozone column, UV can be expected to decrease in mid-latitudes and increase in the tropics (Butler et al., 2016; Lamy et al., 2019). Therefore, climate change, linked to the accumulation of greenhouse gases in the atmosphere, is also one of the phenomena identified to explain the increasing levels of exposure to UV radiation in the tropics.

The western Indian Ocean is mainly located in the tropical region of the southern hemisphere. This part of the world is therefore potentially impacted by the changes in radiation described above. However, this geographical area suffers from a very large measurement deficit, both for ozone and UV radiation on the ground. Studies associated with these topics are sparse in the literature. The originality of Reunion Island is that it is located in the heart of this region and and has benefited from high-quality measurements of ozone and aerosols for several decades thanks to OPAR (Reunion's Atmospheric Physics Observatory). Within the framework of various programmes funded by Europe, Reunion Council or CNES (French Space Agency), the University of Réunion Island has developed a specialized network for the measurement of UV radiation and cloud cover in the south-western part of the Indian Ocean, known as the UV-Indien network. The data-sets presented here are original and, as mentioned, concern an extremely poorly measured region of the globe, which highlights their importance. They include the UV index at 9 stations, the cloud fraction measured at 4 stations. These measurements are ideally suited for assessing the effect of UV radiation on the health of people or ecosystems in this region.

2 Data

2.1 UV-Indien Network

This network currently has 9 stations in 5 countries of the Region (France, Madagascar, Seychelles, Comoros and Mauritius), with 8 scientific, institutional or meteorological partners:

https://doi.org/10.5194/essd-2021-55
Preprint. Discussion started: 3 March 2021

- LACy, Université de la Réunion, Réunion
- IOGA, Institut de Géophysique d'Antananarivo, Madagascar
- Institut Supérieur de Technologie de Diego Suarez, Madagascar
- OPAR, Observatoire de Physique de l'Atmosphère de la Réunion
- Seychelles Meteorological Authority (SMA), Mahé, Seychelles
- Agence Nationale de l'Aviation Civile et de la Météorologie, Moroni, Comores.
- L'université des Comores, Moroni, Comores
- Terre Australes et Antarctiques Françaises, St Pierre, France

Since April 2020, all stations for UVR measurements (one station at Rodrigues, two stations at Réunion, one station at Mahé, three stations at Madagascar, on station Juan de Nova and one station at Moroni) are operational, as are 4 stations for cloud cover measurements (see Table 1 and Figure 1).

All stations are now equipped with a Kipp & Zonen UVS-E-T broadband radiometer. Reunion Island is also equipped with a Bentham UV spectroradiometer. The raw UV measurements obtained by the radiometers are reprocessed considering the calibrations and TOC measured simultaneously. The broadband radiometers will be calibrated every 2 years at the Moufia super site (University of Reunion Island, St Denis) using the Bentham UV spectrometer, itself calibrated every 3 months (Brogniez et al., 2016). The radiometer located at Saint-Denis was previously calibrated at Davos but is now calibrated using the Bentham measurements (Table 3). The TOC correction uses the total ozone measurements made with the UV-Visible spectrometer SAOZ (Pastel et al., 2014; Toihir et al., 2015) on a smaller mesh size (due to the high cost of the instrument and also to the lower variability of ozone). For sites without local total ozone measurements, the TOC given by the OMI satellite is used. Currently, only sites in Reunion and Mahé are equipped with a SAOZ and there are plans to install a new one in Moroni (Ngazidja Island) in 2020 (UN Environment Programme under the Vienna Convention, funding acquired). The level 2 data (final data) obtained are archived on an ftp server accessible to all partners. Finally, cloud cover measurements are carried out using the wide-angle total sky imager, SkyCamVision (SCV), manufactured by Reuniwatts (http://www.reuniwatt.com/). The camera acquires hemispherical images between 380 and 440 nm every minute. Cloud fractions (CF) are calculated following a cloud segmentation algorithm. (Liandrat et al., 2017; Breiman, 2001; Long et al., 2006). All the data can be easily downloaded (open data).

The scientific objectives of this network are the following:

- The study of the annual and inter-annual variability of UVR over the whole Western Indian Ocean basin.
- Validation of numerical model outputs for UVR forecasting.

https://doi.org/10.5194/essd-2021-55
Preprint. Discussion started: 3 March 2021


Open Access Earth System Science Data Discussions

- Long-term monitoring of UVR in the context of climate change and projected ozone depletion of 2 to 4% (Lamy et al., 2019).
- Satellite validation. Instruments from Juan, Seychelles, la Réunion and Antananarivo participate in the validation of the Tropospheric Monitoring Instrument (TROPOMI) surface UV product (Lakkala et al., 2020).

The exploitation of the data from the UV-Indien network will allow a fine characterization UV variability in this region of the globe, in both clear and cloudy skies. The importance of such measurements in a region where almost no data are available should be noted. Finally, UV measurements have recently integrated the international GAW UV WOUDC (World Ozone and Ultraviolet Radiation Data Centre) network.

2.2 Satellite Observations and Global Forecasting of UVI

UVI ground-based observations offers high temporal and spectral resolution and precision. However, to study the impact of climate change on the UVI, global estimates of UVI are also needed. Satellites and Global Forecast Models provide such estimates.

To compute the UVI at the surface, the Global Forecast Model uses a radiative transfer model (RTM) or a look-up table generated by an RTM. Multiple parameters are required, such as TOC, aerosols, CF and SZA. To determine the UVI at the surface, satellite UV estimates are calculated using a combination of RTM calculations and measurements. In order to compare ground UVI measurements with the UVI product from satellites or forecast modelling, we have gathered together the multiple datasets presented in Table 2.

The Bentham spectrometer (called UVI-BENTHAM hereafter) and KippZonen Radiometer (called UVI-RADIO hereafter) are the ground-based instruments part of the UV-Indien. These instruments will be compared with satellite surface UV products (TROPOMI, OMUVBG and GOME-2) and forecast model products (CAMS and TEMIS).

The TROPOMI instrument is onboard the Sentinel-5 Precursor (S5P) polar-orbiting satellite launched on 13 October 2017 as part of the EU Copernicus programme. TROPOMI surface UV radiation products include irradiances with daily integrals at four different wavelengths, and dose rates with daily doses for erythema (CIE Standard, 1998) and vitamin D synthesis (Bouillon et al., 2006) action spectra. All parameters are calculated for overpass time, solar noon time, and for clear-sky conditions (no clouds, no aerosols). The TROPOMI UV algorithm (Lindfors et al., 2018) is based on two pre-computed look-up tables (LUTs): The first is used to retrieve the cloud optical depth from the measured 354 nm reflectance. This cloud optical depth, the total ozone column from the TROPOMI level 2 total ozone column product (Garane et al., 2019), the surface pressure, the surface albedo and the SZA are then used as input to the second LUT from which the UV irradiances and dose rates are retrieved. A post-correction for the effect of absorbing aerosols (Arola et al., 2009) is applied to the irradiances. The ground resolution for the UV products is 7.2x3.5 km^2 (5.6x3.5 km^2 since 6 August 2019) at nadir. Only the estimates corresponding to the time of the overpass are chosen here. The UVI estimated in clear-sky conditions and in all-sky conditions will be used in this study and will both be called UVI-TROPOMI for ease of reading. UVI-TROPOMI computed for clear-sky conditions

https://doi.org/10.5194/essd-2021-55
Preprint. Discussion started: 3 March 2021

will be compared against UVI-RADIO or UVI-BENTHAM measured in clear-sky conditions and UVI-TROPOMI computed for all-sky conditions will be compared against UVI-RADIO or UVI-BENTHAM measured in clear-sky conditions.

OMUVBG is a product derived from the Ozone Monitoring Instrument (Levelt et al. (2006), Tanskanen et al. (2007), Arola et al. (2009)). It is based on the Total Ozone Mapping Spectrometer (TOMS) algorithm to retrieve TOC. TOC, measured with OMI, along with climatological albedo, ozone and temperature profile, elevation and SZA are used as input to an RTM to compute a first estimation of the UVI under clear skies. The measured reflectance at 360nm made by the OMI is used to estimate a cloud modification factor (CMF). The CMF represents the attenuation of UV radiation by clouds and non-absorbing aerosols. The clear-sky UVI computed previously is multiplied by the CMF to obtain an estimation of UVI in all-sky conditions (called UVI-OMUVBG hereafter). This estimate corresponds to the satellite overpass time. Absorbing aerosols are only corrected if the aerosol index is higher than 0.5 and if the measured reflectance at 360 nm is lower than 0.15 (Tanskanen et al., 2006). This could lead to overestimation for regions affected by absorbing aerosols (Tanskanen et al., 2007). UVI-OMUVBG computed for clear-sky conditions will be compared against UVI-RADIO or UVI-BENTHAM measured in clear-sky conditions and UVI-OMUVBG computed for all-sky conditions will be compared against UVI-RADIO or UVI-BENTHAM measured in clear-sky conditions.

The offline surface UV is a product derived from the measurements of the GOME-2 instruments on-board the METOP-B and METOP-C satellites. The offline surface UV contains multiple variables related to UV radiation and human health: UVI, integrated UVB and UVA, and daily doses derived from different biological weighting functions (erythema, DNA damage, plant damage and vitamin-D synthesis). TOC and cloud measurements provided by the AC SAF Total Ozone product and the Advanced Very High Resolution Radiometer (AVHRR-3) reflectances are used with an RTM to compute the offline surface UV product (Kujanpää and Kalakoski, 2015). The product is on a regular 0.5 x 0.5° grid and UVI is computed at local solar noon (called UVI-GOME hereafter).

The Integrated Forecasting System (IFS) of the Copernicus Atmosphere Monitoring Service (CAMS) has been providing UV forecasts since 2012 (Bozzo A., 2015). More precisely, it provides the spectral UV with a spectral resolution of 5 nm and the UVI by integrating the spectral UV according to the erythema action spectrum (CIE Standard, 1998). The UV irradiances and UVI are produced in clear-sky and in all-sky conditions (hereafter called UVI-CAMS). For UVI-CAMS, new forecasts are available every 12 hours: the model output has a time step of 3 hours. From the first forecast of the day, which starts and is initialize at 00:00:00, we take the first, second, third and fourth timesteps of the model (00:00:00, 03:00:00:, 06:000:00 and 09:00:00 respectively) and, from the second forecast, which starts at 12:00:00, we take the first, second, third and fourth timesteps (12:00:00, 15:00:00:, 18:000:00 and 21:00:00 respectively). The horizontal resolution was approximately 80 km prior to 2016-06-21 and approximately 40 km afterwards. Following its continuous development, the CAMS model has been upgraded every year with components that significantly change the UVI forecasts. For instance, improved handling of cloudiness (implemented on 2017-01-24) and a new extraterrestial UV spectrum (implemented on 2017-09-26) have resulted in significant improvements (W. Wandji, 2018). As these changes only affect the data following the upgrade, the CAMS UV forecast is not a homogeneous time series, but should be considered as an evolving UV product with which measurements can be compared. More information on the IFS and CAMS-IFS models is available at https://atmosphere.copernicus.eu/node/326.

https://doi.org/10.5194/essd-2021-55
Preprint. Discussion started: 3 March 2021

UVI-CAMS computed for clear-sky conditions will be compared against UVI-RADIO or UVI-BENTHAM measured in clear-sky conditions and UVI-CAMS computed for all-sky conditions will be compared against UVI-RADIO or UVI-BENTHAM measured in clear-sky conditions.

The TEMIS UVI product is derived from the TOC at solar noon obtained by satellites (SCIAMACHY, GOME-2A or GOME-2B depending on the time period. Following the parameterization of Allaart et al. (2004), a first estimate of UVI is computed with the TOC. The final UVI under clear sky at local solar noon (called UVI-TEMIS hereafter) is obtained by correcting the first estimates for the effects of the Earth-Sun distances, surface albedo, elevation and aerosols (Zempila et al., 2017). The spatial resolution is 0.5 x 0.5°.

Figure 2 represents the time period covered by all datasets at St-Denis. TEMIS shows the longest period covered as of 2002. TROPOMI is the most recent instrument and the UVI data starts at the end of 2017. For the ground-based instruments, UVI-BENTHAM has been acquiring data since 2009 and UVI-RADIO since the end of 2016.

3 Validation

3.1 Calibration

The UV-Indien project is deploying broadband radiometers at various sites in the Indian Ocean. In order to recalibrate these radiometers with a frequency of about 2 years, we plan to regularly reposition the radiometers on the Moufia super measurement site (University of Reunion Island - 20.902°S, 55.485°E), and thus co-locate with the BENTHAM spectrometer, for a period of 3 or 4 months. For the recent recalibration of the UVS-E-T 15-0124, located in St-Denis, the absolute differences (AD) of the UVI, the relative differences (RD) between the UVI measured by the radiometer and the UVI measured by BENTHAM were calculated. These differences are calculated per SZA band (+- 5°) and for clear-sky conditions. We noted that the differences depend on the SZA. As the SZA increases, the absolute values of the UVI tend to decrease and, therefore the absolute difference also tends to decrease. Nonetheless, the RD increases as the SZA increases. This behaviour is observed for all radiometers currently compared to the Bentham (Table 3). While the UVS-E-T radiometer tends to overestimate UVI between 0° and 50° of SZA, the SUV-E radiometer underestimates the UVI. The underestimation is greatest at high SZA. The SUV-E radiometers were installed colocally during the austral winter, when the SZA takes higher values. The differences with respect to the BENTHAM spectroradiometer were used as a reference to recalibrate the KZ Radiometers (UVI-RADIO). UVI-BENTHAM is cosine corrected, its temperature is stabilized and the instrument is regularly calibrated against standard 1000 W lamps, whose origin can be traced to the National Institute of Standards and Technology (Brogniez et al., 2016). We compared both measurements again for all-sky conditions. We noted that the ADs between each radiometer and the BENTHAM were less than 0.5 . RDs were less than 5 to 10% except for the UVS-E-T 15-0124 around 25° of SZA, where the differences could reach about 11%. There was still a SZA dependency: as SZA increased, RD tended to increase, but the magnitude of this effect decreased after recalibration. Note that the radiometers installed in Mahé, Anse Quitor, and Antananarivo are still under the constructor's calibration and have not yet been compared to BENTHAM. These radiometers should be recalibrated during the coming year. Table 4 presents the different radiometers and their current locations, along with the date of the next calibration.

https://doi.org/10.5194/essd-2021-55
Preprint. Discussion started: 3 March 2021

3.2 Comparison of UV-OI Ground Based Measurements, Satellite Estimates and Modelling Estimates of UVI.

Ground-based UVI measurements from the UV-Indien Network were compared with satellite estimates and model UVI estimates. To do this, for each station we took the nearest model grid point or satellite pixel. Then, for each satellite or model estimates computed at this point, we looked for the closest UVI-BENTHAM or UVI-RADIO measurement. Finally, for each couple of measurements we checked the following requirements: the time difference between the estimate and the reference must be less than 5 minutes and the SZA difference must be less than 5 degrees. For these comparisons, the UVI-BENTHAM was also scaled up and linearly interpolated at a resolution of 5 min. For data from the OMUVBG and TROPOMI product, we selected UVI estimates located within 10 km away of the corresponding ground-based station. For CAMS, we took the closest grid point available for each station: 14.8, 9.6, 7.2 and 4.7 km from Antananarivo, Anse Quitor, Mahé and St-Denis respectively. For TEMIS, we took the closest grid point available for each station: 7.8, 13.0, 12.1 and 11.8 km from Antananarivo, Anse Quitor, Mahe and St-Denis respectively. Here, it was chosen to compare the satellite product or model forecast to four stations of the UV Indien Network (Antananarivo, Anse Quitor, Mahé and St-Denis) that have the longest time periods covered. Figure 2 shows the period covered by each data set at these four stations. BENTHAM has been collecting data since 2009 but, in this study, only the period between 2016 and now was chosen because the radiometers were only installed in 2016 or later (in 2017) depending on the stations. The Pearson correlation coefficient and absolute and relative differences were calculated for each ground-based instrument installed at each station. Then, the means and medians of the absolute and relative differences between ground-based measurements and the satellite or model estimates were computed (called M-AD, MED-AD, M-RD and MED-RD hereafter).

The correlation between the BENTHAM at St-Denis and the other measurements is shown in Figure 3. The clear-sky measurements made by BENTHAM have been distinguished and are shown as blue crosses while the measurements for all-sky conditions are shown as red circles. The distribution of the data is represented on the histogram to the right and at the top of each sub-figure. All data sets are well correlated with the UVI-BENTHAM under clear sky conditions; Pearson correlation coefficients are greater than 0.9, except for OMUVBG (0.55) at Saint-Denis. Correlation results for the radiometers at St-Denis, Antananarivo, Mahé and Anse Quitor stations are available in the appendix (Figure A1, A3, A5 and A7 respectively). Correlation coefficients are greater than 0.8 at all stations except Anse Quitor (for TEMIS and OMUVBG), Mahé (for OMUVBG, GOME and TEMIS) and Saint-Denis (OMUVBG). On average, for all stations combined, OMUVBG is the product with the lowest correlation coefficients while CAMS shows the highest correlation coefficients. Mahé is the station that is least well represented station by most models, with correlation coefficients between 0.19 and 0.9.

The Absolute and Relative Differences between satellite product or forecast model and UVI-BENTHAM at St-Denis are shown in Figure 4 and Table 4. The clear-sky conditions are presented in blue on the boxplot (Figure 4) and the corresponding values are reported in Table 4. The all-sky conditions are presented in red on the boxplot (Figure 4) and the corresponding values are shown in brackets in Table 4. Looking at the median of the absolute differences (MED-AD) under all-sky conditions, it can be seen that all data sets, with the exception of OMUVBG, overestimate UVI relative to the UVI-BENTHAM measurements; median overestimation ranges between 0.21 (TROPOMI) and 0.96 (TEMIS). In clear-sky conditions, the me-

https://doi.org/10.5194/essd-2021-55
Preprint. Discussion started: 3 March 2021

dian absolute differences decrease but a UVI overestimation can still be observed for CAMS (+0.21) and TEMIS (+0.27). The smallest median difference is obtained for GOME (-0.01). UVI-RADIO is expected to be aligned with UVI-BENTHAM since it has been recalibrated with the UVI-BENTHAM measurements, so it will not be discussed further here. The mean of the absolute differences under all-sky conditions ranges from 0.34 +- 2.54 (OMUVBG) to +2.31 +-3.26 (TEMIS). Under clear-sky conditions, this absolute difference is smaller and ranges between -0.25 +- 0.73 (TROPOMI) and 0.47 +- 0.55 (CAMS).

The M-RD under all-sky conditions is between 23.93 +- 82 % (OMUVBG) and +59.73 +- 164% (TEMIS). These means and standard deviations are strongly reduced under clear sky conditions; they are between 0.76 +- 8.66 % (GOME) and 12.33 +- 12.27 (CAMS). Similarly, the MED-RD under all-sky conditions are higher than those obtained under clear-sky conditions.

UVI estimates by satellite or models are closer to instruments measurements in clear-sky conditions observed on the ground. This is mainly due to the spatial resolution and clouds representation. The satellite pixel or model grid point is representative of a 5.6 x 3.7 km region for the better defined satellite (TROPOMI) or a 0.5 deg x 0.5 deg region (55 x 55 km) (GOME, OMI and TEMIS). Thus the cloud cover considered is representative of this entire region but it is not necessarily that directly observed above the ground-based instruments. In addition, the pixels and grid points selected are not perfectly centred on the ground instruments. Finally, the four study sites are located in the tropics, present non-uniform topographic conditions and are very close to the sea (with the exception of Antananarivo). These conditions favour the rapid development of clouds and complicate the estimation of cloud cover over the site by the satellite (Lakkala et al., 2020). Thus the clear-sky conditions observed on the ground may not be the same as those observed by satellites or models. This will induce discrepancy between UVI derived from satellite and modelling and UVI observed at the ground.

For the other stations (Appendix A1 to A8), all satellites and models underestimate the surface UVI (UVI-RADIO) except CAMS at Antananarivo, where UVI-CAMS is just above UVI-RADIO with a mean absolute difference of +0.1. In clear-sky conditions, the MED-AD vary between -0.01 for CAMS in Antananarivo and -6.0 for GOME in Mahé. In all-sky conditions, the MED-AD vary between 0.05 for CAMS in Antananarivo and -4.5 for GOME in Mahé. In clear-sky conditions, the MED-RD vary between -0.5 % for CAMS in Antananarivo and -34.5 % for TROPOMI in Mahé. In all-sky conditions, the MED-RD vary between 15.8 % for CAMS in St-Denis and -32.7 % for TROPOMI in Mahé In clear-sky conditions, the M-AD vary between 0.1 for CAMS in Antananarivo and -5.8 for GOME in Mahé. In all-sky conditions, the M-AD vary between 0.2for CAMS in Antananarivo and -3.5 for TROPOMI and GOME in Mahé. In clear-sky conditions, the M-RD vary between -10.9 % for CAMS in Antananarivo and 56.15% for TEMIS in Anse Quitor. In all-sky conditions, the M-RD vary between -25,0% for TROPOMI in Mahé and 26.4 % for TEMIS in Mahé.

Although TROPOMI has large relative differences, especially in Mahé, it is also the product with the most consistent differences. The relative and absolute standard deviation is the smallest at all stations. It should be noted that all satellite or model estimates give poor results at the Mahé station. An examination of percentage of clear days showed that, in Mahé, Anse Quitor and Antananarivo, there are only 16% clear days while, in St-Denis, there are 27% clear days. In addition, Anse Quitor and Antananarivo radiometers have a 1 min resolution, while those in Mahé and St-Denis have a 5 min resolution. The small number of clear-sky days combined with the larger temporal resolution reduce the number of points compared in clear-sky conditions at Mahé. For OMUVBG, TROPOMI, GOME and TEMIS, which produce only one UVI estimate per day, the number of points

https://doi.org/10.5194/essd-2021-55
Preprint. Discussion started: 3 March 2021

compared ranges from 72 to 253. Mahé station is also closer to the equator than the other stations (at about -4 South) and is strongly influence by the convection in this region.

Outliers and large differences could be due to numerous issues. The satellite measurements and the modelled UVI do not have spatial resolutions that can accurately represent the sky conditions just above the ground-based instruments. The satellite or model grid points used in this study are either the closest grid point to the station or the average of four grid points encircling the station location. Nonetheless, for satellite estimates or model results, spatial resolution can be as high as 50km (TEMIS or GOME) or as low as 3.7km (TROPOMI). Also, cloud conditions, albedo or altitude can vary strongly over distances smaller than 100km. These differences can affect the quality of the model forecast or of the inversion algorithm used by the satellite. Differences between a satellite product or model forecast and radiometers measurements could also be explained by a drift in the radiometer calibration. The recalibration of radiometers in Antananarivo, Anse Quitor and Mahé is planned for early 2021. Nevertheless, UVI-BENTHAM, which provides high quality data and is recalibrated every 3 months, still shows a MED-RD between -2.5% (TROPOMI) and 11.3% (CAMS), and a MED-AD between -0.2 (TROPOMI) and 0.3 (TEMIS), in clear-sky conditions.

Correlation, boxplot and tables for UVI-RADIO at St-Denis, Antananarivo, Mahé and Anse Quitor are available in supplements (Appendix Figures A1 to A8 and appendix Tables A1 to A4).

4 First Results of the UV-Indien project

4.1 UVI Climatology

For each station, the UVI variability, as measured by the radiometers, was studied. The diurnal cycle of UVI was calculated for the whole measurement period. The results are presented on Figure 5: the mean UVI (blue line), the UVI maximum (continuous red line) and the first and third quartiles (blue shading) of the UVI in all-sky conditions during the day are represented for Antananarivo, Mahé, Anse Quitor and St-Denis. For the same station, in clear-sky conditions, the mean UVI is represented by a green line, the maximum UVI by a dashed red line and quartiles by shades of green.

In all-sky conditions, the mean UVI at local solar noon varies from about 10 (Antananarivo, Anse Quitor, St-Denis) to about 14 (Mahé). The difference between Mahé and the other three stations can be explained by the latitude of the stations: Antananarivo, Anse Quitor and St-Denis are at about 20° South while Mahé is at 4.6° South. Therefore, in Mahé, SZA are lower throughout the year, which induces a higher UVI during the year. For clear-sky conditions, the mean UVI is higher than for all-sky conditions at all stations. In addition, the first and third quartiles are closer to the mean in clear-sky conditions. This is due to the impact of cloud attenuation on UVI variability.

It can be seen that the UVI maxima can be higher than 20 for Anse Quitor, Antananarivo and Mahé. For St-Denis, the UVI maxima can reach 16. The highest UVIs are observed at the Mahé station with maxima of up to 25. At all stations, the UVI maxima are higher for all-sky conditions than clear-sky conditions. These maximas of UVI, in all-sky conditions, can be 1 to 4 higher than maxima in clear-sky conditions. This is due to the enhancement of UVI by fractional cloud cover, which can produce multiple scattering, thus enhancing the UVI on the surface. This phenomenon was previously observed at

https://doi.org/10.5194/essd-2021-55
Preprint. Discussion started: 3 March 2021

St-Denis (Lamy et al., 2018). The largest differences between the maxima in all-sky conditions and clear-sky conditions are observed at Mahé, the lowest differences are observed at St-Denis and Anse Quitor. Antananarivo also shows a significant UVI enhancement, by about 2 to 3. Antananarivo is at a higher altitude than the other three stations, at about 1.3 km asl. The city is also located inland and suffers from heavy pollution. Therefore, both aerosols and altitude can be expected to have a significant impact on the variability of surface UVIs.

In Antananarivo, the peaks of UVI mean and maxima are aligned for both clear-sky and all-sky conditions. In St-Denis the peak of mean UVI occurs later in the day for clear-sky conditions than for to all-sky conditions. In Anse Quitor, the peak of UVI is early in the day. This is due to the time zone used at Anse Quitor. Rodrigues Island, where Anse Quitor is located, shares the same time zone as St-Denis (Reunion island) or Mahé (Seychelles) but is farther east by about 8 degrees of longitude. In Mahé, the peaks of mean UVI, in all-sky and clear-sky conditions, are aligned. This is not the case for the maxima, which occur 1 to 2 hours earlier in all-sky conditions than in clear-sky conditions. The position of the UVI peaks can be explained by the variability of the cloud cover as will be shown in the next section.

The average monthly climatology of the daily UVI maximum and the daily UVI at solar noon were also calculated. Although the datasets do not cover a sufficient period to be climatologically significant, the annual variability and the differences between UVI and UVI daily maxima at solar noon present interesting results. Figure 6 shows these monthly climatologies for the four stations of Antananarivo, St-Denis, Mahé and Anse Quitor. The daily maxima of UVI are in red lines with filled circles, the corresponding sun zenith angles are in orange dashed lines with filled circles. The UVIs at local solar noon are marked with blue lines and crosses, the corresponding sun zenith angles are shown as dashed orange lines with crosses.

For all stations and all months of the year, the maximum daily UVI (UVI_{DMAX}) is higher than the average UVI at solar noon (UVI_{SNOON}). These climatologies are based on data sets for all types of cloud cover. Thus, the cloud cover will introduce a bias in the result. UVI_{DMAX} include maxima of UVI during cloud enhancements, which could occur earlier or later than the local solar noon, as discussed in the previous result (Figure 5). UVI_{DMAX} also include maxima of UVI during clear-sky days, which will usually occurs at local solar noon. UVI_{SNOON} will include only UVI at local solar noon with or without cloud cover. This is why UVI_{DMAX} is always higher than UVI_{SNOON} in all-sky conditions. The differences range between 1 during austral winter at St-Denis and 6 in austral summer at Mahé. The corresponding SZA differences ranges from 0 to 6 °.

Looking at the few complete clear-sky days revealed a UVI_{SNOON} and a UVI_{DMAX} that were almost equivalent. However, as there were not enough clear sky measurements per month and per SZA bin, these results are not represented here.

4.2 Cloud measurements

Early results from the camera are able to describe the mean diurnal cloud cycles over each station. Figure 7a shows the mean diurnal cycle of the cloud fraction (CF) over Antananarivo for the entire year (black curve), along with the distribution of the first and third quartiles (blue shaded area). Seasonal means of CF are also presented for December, January and February (DJF, in green), March, April and May (MAM, in red), September, October and November (SON, in orange) and June, July and August (JJA, in purple). The density of the corresponding data set for each month of the year is represented in Figure

https://doi.org/10.5194/essd-2021-55
Preprint. Discussion started: 3 March 2021


Open Access Earth System Science Data Discussions

7b. Figure 7c represents the difference of UVI maxima between clear-sky UVI and all-sky UVI for the same period. The UVI distribution is also available in Figure 6d. The same results are presented for St-Denis on Figure 8.

Over Antananarivo (Figure 7), the annual mean diurnal cycle shows intermediate values of CF, of about 0.6 at the beginning of the the day. CF tends to decrease during the day and to increase in the late afternoon. Antananarivo is located in a mountainous region in the high lands of Madagascar at 1370m asl. The difference in CF in the four seasons is not statistically significant, especially for the JJA and SON seasons. Since the camera at Antananarivo was installed in April, 2019, there are not yet significant numbers of data points for certain months of the year. Nonetheless, since the radiometers at Antananarivo were installed in 2016, there is a significant number of UVI data over the whole year (Figure 7d). The largest difference between maxima of UVI in clear-sky conditions and maxima of UVI in all-sky conditions can be observed for the DJF and JJA seasons (Figure 7c). CF diurnal profiles are quite different between the DJF season and the JJA season, with DJF showing CF higher than the annual mean while JJA shows CF lower than the annual mean. The CF diurnal cycle alone is probably not the only factor involved in triggering UVI enhancement: cloud distributions and type of clouds probably play a role in UVI enhancement (Sabburg and Wong, 2000; Calbó et al., 2005).

Over St-Denis the mean diurnal CF cycle shows a different profile from that of Antananarivo. CF values are lower in the morning, at around 0.4, and increase during the day to reach 0.6. St-Denis is located on the northern part of Reunion Island, a mountainous island under the influence of the south-east trade winds which induce cloud formation on the southern part of the island during the morning. During the day, the clouds tend to overflow over the rest of the island, thus inducing a rising CF during the day. The lowest values of CF throughout the day are observed in SON. DJF, MAM and JJA follow the annual mean. For this station, well spread CF and UVI data are available throughout the year (Figure 8b and 8d). A glance at the difference between the maxima of UVI in clear-sky conditions and the maxima of UVI in all-sky conditions (Figure 7c), shows that almost all the highest differences are observed for the DJF season. These differences can reach -2.4. The JJA season also shows large differences during the morning but, after 10 am, the differences are lower than in DJF season most of the time. 10 am is also the hour when the CF starts to rise more rapidly in JJA (Figure 7a). This result could indicate than UVI enhancement occurs less frequently above a certain CF threshold.

The cameras of the UV-Indien network present promising results for studying cloud variability and its impact on UV radiation in the Indian Ocean region. CF alone is probably not sufficient to give an understanding UVI enhancement. Cloud types, types of cloud distribution and solar occultation by clouds also need to be considered. Moreover, the UV Indien Network is very young, so there is not yet enough data to conduct significant climatological studies.

5 Data Availability

Data from the UV radiometers and the total sky imagers can be downloaded from Zenodo and are referenced under the following doi: https://doi.org/10.5281/zenodo.4572026 (Lamy and Portafaix, 2021).

https://doi.org/10.5194/essd-2021-55
Preprint. Discussion started: 3 March 2021

The data from the UV radiometers are also available on the WOUDC website at these addresses for the four stations studied here :

- Saint-Denis, La Réunion : https://woudc.org/data/stations/?id=530
- Mahé, Seychelles : https://woudc.org/data/stations/?id=207
- Anse Quitor, Mauritius : https://woudc.org/data/stations/?id=532
- Antananarivo, Madagascar : https://woudc.org/data/stations/?id=531

The TROPOMI surface UV radiation product used in this study is available at https://nsdc.fmi.fi/data/data_s5puv.php
The AC SAF (GOME/METOP) data can be downloaded through the website at https://acsaf.org
The TEMIS data can be downloaded through the website at http://www.temis.nl/uvradiation/UVindex.html
The OMUVBG data can be downloaded through the website at https://disc.gsfc.nasa.gov/datasets/OMUVBG_003
The CAMS data can be downloaded through the website at https://apps.ecmwf.int

6 Conclusions

The ground-based spectroradiometer and radiometer of the UV-Indien network were compared with satellites estimates and the estimates of the UVI model. The correlation coefficient between the satellite or model estimates and the ground-based measurements was greater than 0.9 at all stations except Mahé and for all datasets except OMUVBG. In all-sky conditions, the largest UVI median absolute difference between the satellite or model estimates and the ground-based instruments was -0.4 (TROPOMI), -1.4(TROPOMI), -2.3(GOME) and -6.0(GOME) at St-Denis, Antananarivo (), Anse Quitor and Mahé respectively. In clear-sky conditions, the largest UVI median absolute difference between the satellites or model estimates and the ground-based instruments was 1.1(TEMIS), -1.3(TROPOMI), -1.7(GOME) and -4.6 (GOME) at St-Denis, Antananarivo, Anse Quitor and Mahé respectively. In all-sky conditions, the smallest UVI median difference between the satellites or model estimates and the measurements of ground-based instruments was 0.1 (CAMS and TEMIS), -0.1 (CAMS), -0.1 (CAMS) and 0.1 (CAMS) at St-Denis, Antananarivo, Anse Quitor and Mahé respectively. In clear-sky conditions, the smallest UVI median difference between the satellites or model estimates and the measurements of ground-based instruments was 0.02 (TROPOMI), 0.04 (OMUVBG), -0.1 (CAMS) and -0.4 (CAMS) at St-Denis, Antananarivo, Anse Quitor and Mahé respectively. Compared to ground measurements, UVI-CAMS showed the most consistent results at all stations in both all-sky and clear-sky conditions. At St-Denis, satellite and model estimates were usually found to overestimate UVI compared to ground-based instruments, while at Antananarivo, Anse Qutor and Mahé, satellite and model were found to underestimate ground-based measurements of UVI.

The largest discrepancies were observed at the Mahé station. Many reasons can be evoked to explain these differences. The satellite or model resolution may not be able to accurately determine the sky conditions above the station. As Mahé is under

https://doi.org/10.5194/essd-2021-55
Preprint. Discussion started: 3 March 2021

the influence of the sea-breeze, the formation of clouds is frequent late in the morning. From the ground, these clouds could be seen to induce irradiance enhancements due to multiple scattering at their edges. From the satellite's point of view, only strong backscattering would be observed and an attenuation of the clouds would therefore be applied to the UV product. This is also consistent with the time of the satellite estimates (solar-noon or overpass), which is late in the morning when cloud formation is frequent which would induce backscattering. UVI enhancement occurs also frequently during this time (Figure 5). This two phenomenons could explain both the observed high UVI and the discrepancy with satellite and model estimates. A drift in the radiometer calibration could also explain part of the difference. Mahé also presents a low number of clear-sky comparison points since the K&Z radiometer temporal resolution is 5 min and there are only 16% of clear-sky days. St-Denis and Anse Quitor are mountainous islands also under the influence of trade winds, where there is also frequent cloud formation in the late morning. A fractional cloud sky cover could induce UVI enhancements measured by the ground-based instruments while satellites and model could apply attenuation of the measured UVI instead. These two stations are located at about 20 degrees south, while Mahé is located at about 5 degrees south. Therefore, the maxima of UVI are higher at Mahé and the resulting enhancement of UVI should also be stronger. To investigate the impact of clouds on UVI, all-sky cameras have recently been deployed at each station of the UV Indien network. When a significant number of data have been be acquired, another study will address the subject of clouds and UV in the tropics.

We also analysed the UVI variability at these different sites. Mean UVI at local solar noon ranges between 10 (Antananarivo, Anse Quitor, St-Denis) and about 14 (Mahé, Seychelles). While the mean UVI in clear-sky conditions are higher than mean UVI in all-sky conditions, the UVI maxima in all-sky conditions are higher than in clear-sky conditions. This phenomenon of UVI enhancement by clouds can be observed at the four stations studied here. Measurements of the diurnal cloud fraction cycle have also been studied, enabling different daily profiles to be distinguished depending on the station and the season. However, these data are still recent and there are not enough measurements available at present to give a significant statistical description. The highest UVI enhancement is observed at Mahé where there is a 4 to 5 UVI unit difference between maxima of UVI in all-sky conditions compared to clear-sky conditions. When the number of cloud fraction measurements is significant throughout the year and the time period covered by the camera is longer, it will be possible to combine Cloud Fraction and UVI data to better understand and quantify the UVI enhancement by clouds. The UVI data at the other 4 sites of UV Indien Network (Maido, Diego-Suarez, Moroni, Fort Dauphin and Juan de Nova) will also be the subject of a future study when sufficient data have been collected.

Acknowledgements. We thank the AC SAF project of EUMETSAT for providing the GOME-2/Metop offline surface UV products used in this paper. We also thank the Finnish Meteorological Institute for providing the TROPOMI UV products, and especially Jukka Kujanpää for product development.

UV-Indien Network is funded jointly by European cooperation programme PO INTERREG-V and the Regional Council of Reunion Island. The BENTHAM spectrometer and UV radiometer at St Denis are managed by the OSU-R and are funded by the INSU/CNRS network and

https://doi.org/10.5194/essd-2021-55
Preprint. Discussion started: 3 March 2021

the University of Reunion Island. The authors thank to Reuniwatt for the support provided during the installation of the total sky cameras at the different sites of the UV-Indien network.

https://doi.org/10.5194/essd-2021-55
Preprint. Discussion started: 3 March 2021

References

Arola, A., Kazadzis, S., Lindfors, A., Krotkov, N., Kujanpää, J., Tamminen, J., Bais, A., di Sarra, A., Villaplana, J. M., Brogniez, C., Siani, A. M., Janouch, M., Weihs, P., Webb, A., Koskela, T., Kouremeti, N., Meloni, D., Buchard, V., Auriol, F., Ialongo, I., Staneck, M., Simic, S., Smedley, A., and Kinne, S.: A new approach to correct for absorbing aerosols in OMI UV, Geophysical Research Letters, 36, https://doi.org/10.1029/2009GL041137, https://agupubs.onlinelibrary.wiley.com/doi/abs/10.1029/2009GL041137, 2009.

Bernhard, G. H., Neale, R. E., Barnes, P. W., Neale, P., Zepp, R. G., Wilson, S. R., Andrady, A. L., Bais, A. F., McKenzie, R., Aucamp, P., et al.: Environmental effects of stratospheric ozone depletion, UV radiation and interactions with climate change: UNEP Environmental Effects Assessment Panel, update 2019, Photochemical & Photobiological Sciences, 19, 542–584, 2020.

Bouillon, R., Eisman, J., Garabedian, M., Holick, M., Kleinschmidt, J., Suda, T., Terenetskaya, I., and Webb, A.: Action Spectrum for the Production of Pre-vitamin D3 in Human Skin: CIE 174-2006, Wien, Austria: International Commission on Illumination, 2006.

Bozzo A., Arola A., C. V. P. M.: Report on implementation of spectral UV irradiance, MACC-III deliverable D57.2, work package 122, Tech. rep., 2015.

Breiman, L.: Random forests, Machine learning, 45, 5–32, 2001.

Brogniez, C., Auriol, F., Deroo, C., Arola, A., Kujanpää, J., Sauvage, B., Kalakoski, N., Pitkänen, M. R. A., Catalfamo, M., Metzger, J.-M., and et al.: Validation of satellite-based noontime UVI with NDACC ground-based instruments: influence of topography, environment and satellite overpass time, Atmospheric Chemistry and Physics, 16, 15 049–15 074, https://doi.org/10.5194/acp-16-15049-2016, http://dx.doi.org/10.5194/acp-16-15049-2016, 2016.

Butchart, N.: The Brewer-Dobson circulation, Reviews of Geophysics, 52, 157–184, https://doi.org/10.1002/2013rg000448, 2014.

Butler, A. H., Daniel, J. S., Portmann, R. W., Ravishankara, A. R., Young, P. J., Fahey, D. W., and Rosenlof, K. H.: Diverse policy implications for future ozone and surface UV in a changing climate, Environmental Research Letters, 11, 064 017, http://stacks.iop.org/1748-9326/11/i=6/a=064017, 2016.

Cadet, J.-M., Portafaix, T., Bencherif, H., Lamy, K., Brogniez, C., Auriol, F., Metzger, J.-M., Boudreault, L.-E., and Wright, C. Y.: Inter-Comparison Campaign of Solar UVR Instruments under Clear Sky Conditions at Reunion Island (21°S, 55°E), International Journal of Environmental Research and Public Health, 17, 2867, https://doi.org/10.3390/ijerph17082867, 2020.

Calbó, J., Pagès, D., and González, J.-A.: Empirical studies of cloud effects on UV radiation: A review, Reviews of Geophysics, 43, https://doi.org/10.1029/2004RG000155, https://agupubs.onlinelibrary.wiley.com/doi/abs/10.1029/2004RG000155, 2005.

Chipperfield, M. P., Dhomse, S. S., Feng, W., McKenzie, R., Velders, G. J., and Pyle, J. A.: Quantifying the ozone and ultraviolet benefits already achieved by the Montreal Protocol, Nature communications, 6, 1–8, 2015.

CIE Standard, C.: Erythema reference action spectrum and standard erythema dose, CIE S, 7, E1998, 1998.

Duan, S.-M., Zhao, X.-S., Wen, R.-F., Huang, J.-J., Pi, G.-H., Zhang, S.-X., Han, J., Bi, S.-L., Ruan, L., Dong, X.-P., and SARS Research Team: Stability of SARS coronavirus in human specimens and environment and its sensitivity to heating and UV irradiation, Biomedical and environmental sciences : BES, 16, 246—255, http://europepmc.org/abstract/MED/14631830, 2003.

Eyring, V., Lamarque, J.-F., Hess, P., Arfeuille, F., Bowman, K., Chipperfiel, M. P., Duncan, B., Fiore, A., Gettelman, A., Giorgetta, M. A., et al.: Overview of IGAC/SPARC Chemistry-Climate Model Initiative (CCMI) community simulations in support of upcoming ozone and climate assessments, SPARC newsletter, 40, 48–66, 2013.

Garane, K., Koukouli, M.-E., Verhoelst, T., Lerot, C., Heue, K.-P., Fioletov, V., Balis, D., Bais, A., Bazureau, A., Dehn, A., Goutail, F., Granville, J., Griffin, D., Hubert, D., Keppens, A., Lambert, J.-C., Loyola, D., McLinden, C., Pazmino, A., Pommereau, J.-P., Redondas,

https://doi.org/10.5194/essd-2021-55
Preprint. Discussion started: 3 March 2021

A., Romahn, F., Valks, P., Roozendael, M. V., Xu, J., Zehner, C., Zerefos, C., and Zimmer, W.: TROPOMI/S5P total ozone column data: global ground-based validation and consistency with other satellite missions, Atmospheric Measurement Techniques, 12, 5263–5287, https://doi.org/10.5194/amt-12-5263-2019, 2019.

Herman, J. R., Labow, G., Hsu, N. C., and Larko, D.: Changes in cloud and aerosol cover (1980-2006) from reflectivity time series using SeaWiFS, N7-TOMS, EP-TOMS, SBUV-2, and OMI radiance data, Journal of Geophysical Research: Atmospheres, 114, https://doi.org/10.1029/2007JD009508, 2009.

Kinne, S., O'Donnel, D., Stier, P., Kloster, S., Zhang, K., Schmidt, H., Rast, S., Giorgetta, M., Eck, T. F., and Stevens, B.: MAC-v1: A new global aerosol climatology for climate studies, Journal of Advances in Modeling Earth Systems, 5, 704–740, https://doi.org/10.1002/jame.20035, 2013.

Krotkov, N. A., Bhartia, P. K., Herman, J. R., Fioletov, V., and Kerr, J.: Satellite estimation of spectral surface UV irradiance in the presence of tropospheric aerosols: 1. Cloud-free case, Journal of Geophysical Research: Atmospheres, 103, 8779–8793, https://doi.org/10.1029/98JD00233, http://dx.doi.org/10.1029/98JD00233, 1998.

Kujanpää, J. and Kalakoski, N.: Operational surface UV radiation product from GOME-2 and AVHRR/3 data, Atmospheric Measurement Techniques, 8, 4399–4414, https://doi.org/10.5194/amt-8-4399-2015, 2015.

Lakkala, K., Kujanpää, J., Brogniez, C., Henriot, N., Arola, A., Aun, M., Auriol, F., Bais, A. F., Bernhard, G., De Bock, V., Catalfamo, M., Deroo, C., Diémoz, H., Egli, L., Forestier, J.-B., Fountoulakis, I., Garcia, R. D., Gröbner, J., Hassinen, S., Heikkilä, A., Henderson, S., Hülsen, G., Johnsen, B., Kalakoski, N., Karanikolas, A., Karppinen, T., Lamy, K., León-Luis, S. F., Lindfors, A. V., Metzger, J.-M., Minvielle, F., Muskatel, H. B., Portafaix, T., Redondas, A., Sanchez, R., Siani, A. M., Svendby, T., and Tamminen, J.: Validation of TROPOMI Surface UV Radiation Product, Atmospheric Measurement Techniques Discussions, 2020, 1–37, https://doi.org/10.5194/amt-2020-121, https://www.atmos-meas-tech-discuss.net/amt-2020-121/, 2020.

Lamy, K. and Portafaix, T.: Ultraviolet Index measurements in the Indian Ocean, https://doi.org/10.5281/zenodo.4572026, https://doi.org/10.5281/zenodo.4572026, 2021.

Lamy, K., Portafaix, T., Brogniez, C., Godin-Beekmann, S., Bencherif, H., Morel, B., Pazmino, A., Metzger, J. M., Auriol, F., Deroo, C., Duflot, V., Goloub, P., and Long, C. N.: Ultraviolet radiation modelling from ground-based and satellite measurements on Reunion Island, southern tropics, Atmospheric Chemistry and Physics, 18, 227–246, https://doi.org/10.5194/acp-18-227-2018, https://www.atmos-chem-phys.net/18/227/2018/, 2018.

Lamy, K., Portafaix, T., Josse, B., Brogniez, C., Godin-Beekmann, S., Bencherif, H., Revell, L., Akiyoshi, H., Bekki, S., Hegglin, M. I., Jöckel, P., Kirner, O., Liley, B., Marecal, V., Morgenstern, O., Stenke, A., Zeng, G., Abraham, N. L., Archibald, A. T., Butchart, N., Chipperfield, M. P., Di Genova, G., Deushi, M., Dhomse, S. S., Hu, R.-M., Kinnison, D., Kotkamp, M., McKenzie, R., Michou, M., O'Connor, F. M., Oman, L. D., Pitari, G., Plummer, D. A., Pyle, J. A., Rozanov, E., Saint-Martin, D., Sudo, K., Tanaka, T. Y., Visioni, D., and Yoshida, K.: Clear-sky ultraviolet radiation modelling using output from the Chemistry Climate Model Initiative, Atmospheric Chemistry and Physics, 19, 10 087–10 110, https://doi.org/10.5194/acp-19-10087-2019, https://www.atmos-chem-phys.net/19/10087/2019/, 2019.

Levelt, P. F., van den Oord, G. H. J., Dobber, M. R., Malkki, A., Huib Visser, Johan de Vries, Stammes, P., Lundell, J. O. V., and Saari, H.: The ozone monitoring instrument, IEEE Transactions on Geoscience and Remote Sensing, 44, 1093–1101, https://doi.org/10.1109/TGRS.2006.872333, 2006.

Liandrat, O., Cros, S., Braun, A., Saint-Antonin, L., Decroix, J., and Schmutz, N.: Cloud cover forecast from a ground-based all sky infrared thermal camera, in: Remote Sensing of Clouds and the Atmosphere XXII, edited by Comerón, A., Kassianov, E. I., and Schäfer, K., vol.

https://doi.org/10.5194/essd-2021-55
Preprint. Discussion started: 3 March 2021

10424, pp. 19 – 31, International Society for Optics and Photonics, SPIE, https://doi.org/10.1117/12.2278636, https://doi.org/10.1117/12.2278636, 2017.

Lindfors, A. V., Kujanpää, J., Kalakoski, N., Heikkilä, A., Lakkala, K., Mielonen, T., Sneep, M., Krotkov, N. A., Arola, A., and Tamminen, J.: The TROPOMI surface UV algorithm, Atmospheric Measurement Techniques, 11, 997–1008, https://doi.org/10.5194/amt-11-997-2018, 2018.

Long, C. N., Sabburg, J. M., Calbó, J., and Pagès, D.: Retrieving Cloud Characteristics from Ground-Based Daytime Color All-Sky Images, Journal of Atmospheric and Oceanic Technology, 23, 633–652, https://doi.org/10.1175/JTECH1875.1, https://doi.org/10.1175/JTECH1875.1, 2006.

Observatoire Régional de la Santé de La Réunion: Melanome Cutane à la Réunion, 2008.

Pastel, M., Pommereau, J.-P., Goutail, F., Richter, A., Pazmino, A., Ionov, D. V., and Portafaix, T.: Construction of merged satellite total O 3 and NO 2 time series in the tropics for trend studies and evaluation by comparison to NDACC SAOZ measurements, 2014.

Sabburg, J. and Wong, J.: The effect of clouds on enhancing UVB irradiance at the Earth's surface: A one year study, Geophysical Research Letters, 27, 3337–3340, https://doi.org/10.1029/2000GL011683, http://dx.doi.org/10.1029/2000GL011683, 2000.

Sitek, A., Rosset, I., Żądzińska, E., Kasielska-Trojan, A., Neskoromna-Jędrzejczak, A., and Antoszewski, B.: Skin color parameters and Fitzpatrick phototypes in estimating the risk of skin cancer: A case-control study in the Polish population, Journal of the American Academy of Dermatology, 74, 716 – 723, https://doi.org/https://doi.org/10.1016/j.jaad.2015.10.022, http://www.sciencedirect.com/science/article/pii/S0190962215023786, 2016.

Tanskanen, A., Krotkov, N. A., Herman, J. R., and Arola, A.: Surface ultraviolet irradiance from OMI, IEEE Transactions on Geoscience and Remote Sensing, 44, 1267–1271, 2006.

Tanskanen, A., Lindfors, A., Määttä, A., Krotkov, N., Herman, J., Kaurola, J., Koskela, T., Lakkala, K., Fioletov, V., Bernhard, G., and et al.: Validation of daily erythemal doses from Ozone Monitoring Instrument with ground-based UV measurement data, Journal of Geophysical Research, 112, https://doi.org/10.1029/2007jd008830, http://dx.doi.org/10.1029/2007JD008830, 2007.

Toihir, A. M., Bencherif, H., Sivakumar, V., El Amraoui, L., Portafaix, T., and Mbatha, N.: Comparison of total column ozone obtained by the IASI-MetOp satellite with ground-based and OMI satellite observations in the southern tropics and subtropics, Annales Geophysicae, 33, 1135–1146, https://doi.org/10.5194/angeo-33-1135-2015, https://angeo.copernicus.org/articles/33/1135/2015/, 2015.

W. Wandji, M. R. A. Pitkänen, A. A.: UV EQA report 9, September-November 2017,Validation Report of the CAMS UV processor, Tech. rep., ECMWF Copernicus Report, cAMS$72_2015SC2_D72.3.2.1 - 2017SON_UV_VAL_201803_v$, 2018.

WHO: Report of the WMO Meeting of Experts on UV-B Measurements, Data Quality and Standardization of UV Indices (Les Diablerets, 25–28 July, 1994)., 1995.

WMO: Scientific assessment of ozone depletion: 2018, Global Ozone Research and Monitoring Project-Report No. 58, p. 588pp., 2018.

Wright, C. Y., Brogniez, C., Ncongwane, K. P., Sivakumar, V., Coetzee, G., Metzger, J.-M., Auriol, F., Deroo, C., and Sauvage, B.: Sunburn Risk Among Children and Outdoor Workers in South Africa and Reunion Island Coastal Sites, Photochemistry and Photobiology, 89, 1226–1233, https://doi.org/10.1111/php.12123, http://dx.doi.org/10.1111/php.12123, 2013.

Zempila, M.-M., van Geffen, J. H. G. M., Taylor, M., Fountoulakis, I., Koukouli, M.-E., van Weele, M., van der A, R. J., Bais, A., Meleti, C., and Balis, D.: TEMIS UV product validation using NILU-UV ground-based measurements in Thessaloniki, Greece, Atmospheric Chemistry and Physics, 17, 7157–7174, https://doi.org/10.5194/acp-17-7157-2017, 2017.

https://doi.org/10.5194/essd-2021-55
Preprint. Discussion started: 3 March 2021

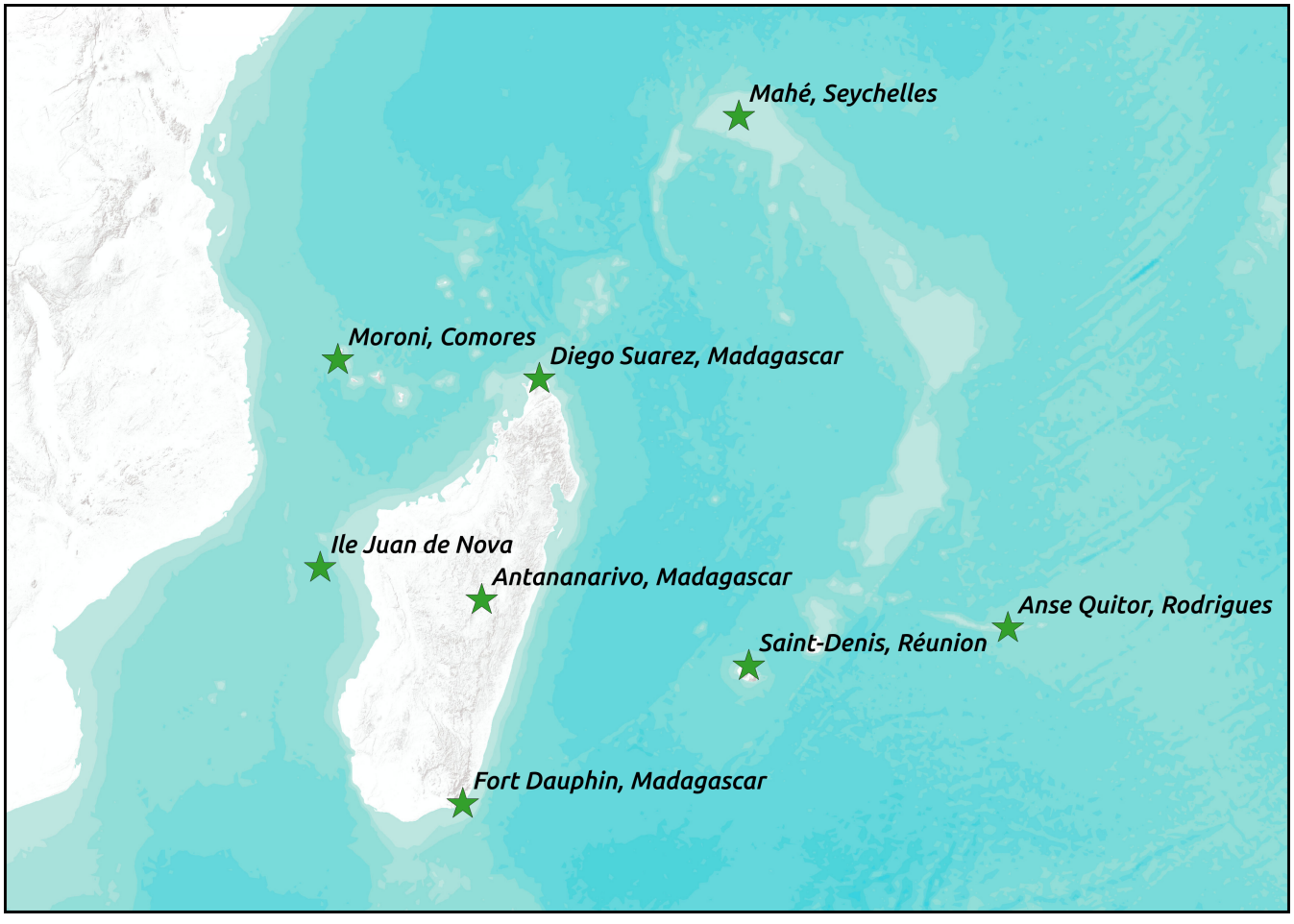

Figure 1. Location of the UV-Indien Stations

https://doi.org/10.5194/essd-2021-55
Preprint. Discussion started: 3 March 2021

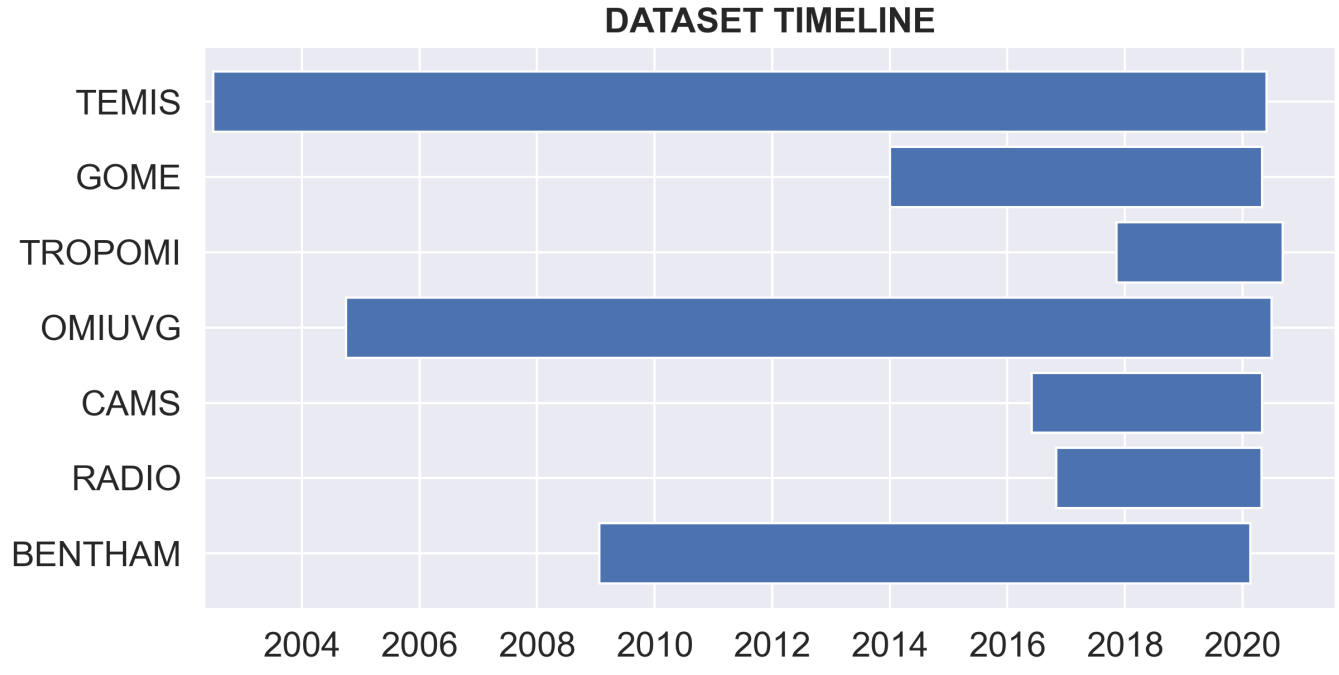

Figure 2. Timeline of the UVI Dataset used in this study

https://doi.org/10.5194/essd-2021-55
Preprint. Discussion started: 3 March 2021

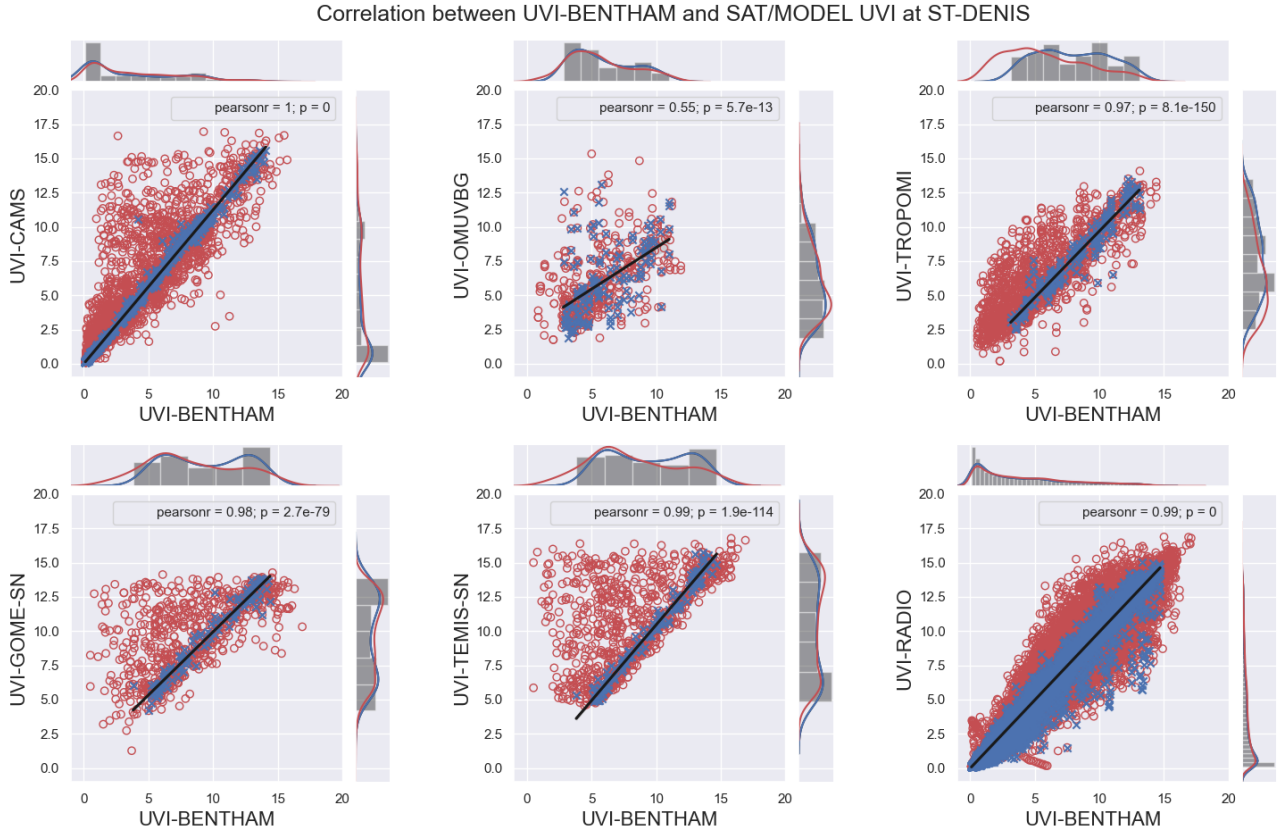

Figure 3. Correlation between UVI-BENTHAM and Sat/Model Estimates at ST-DENIS.

A histogram representing each dataset distribution is represented of the right and at the top side of each subfigure.

https://doi.org/10.5194/essd-2021-55
Preprint. Discussion started: 3 March 2021

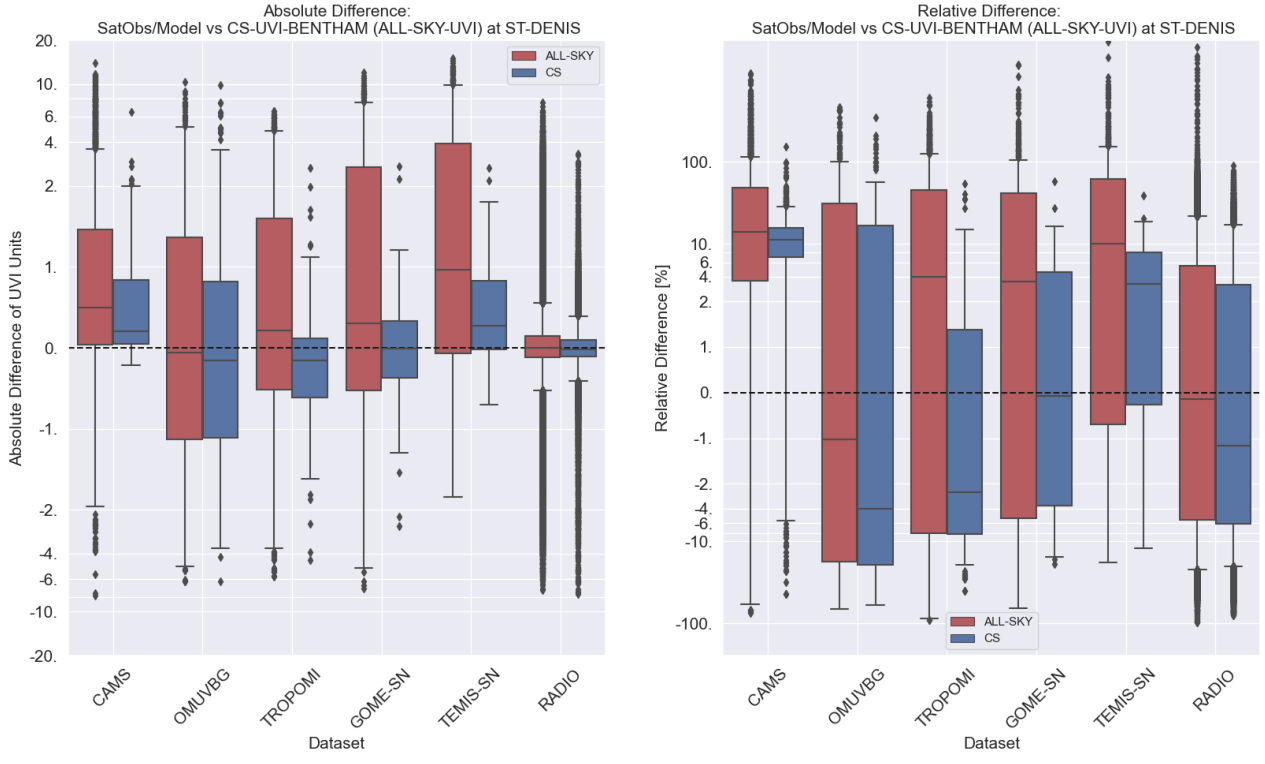

Figure 4. Boxplot of differences between UVI-BENTHAM and Sat/Model Estimates at ST-DENIS.

https://doi.org/10.5194/essd-2021-55
Preprint. Discussion started: 3 March 2021

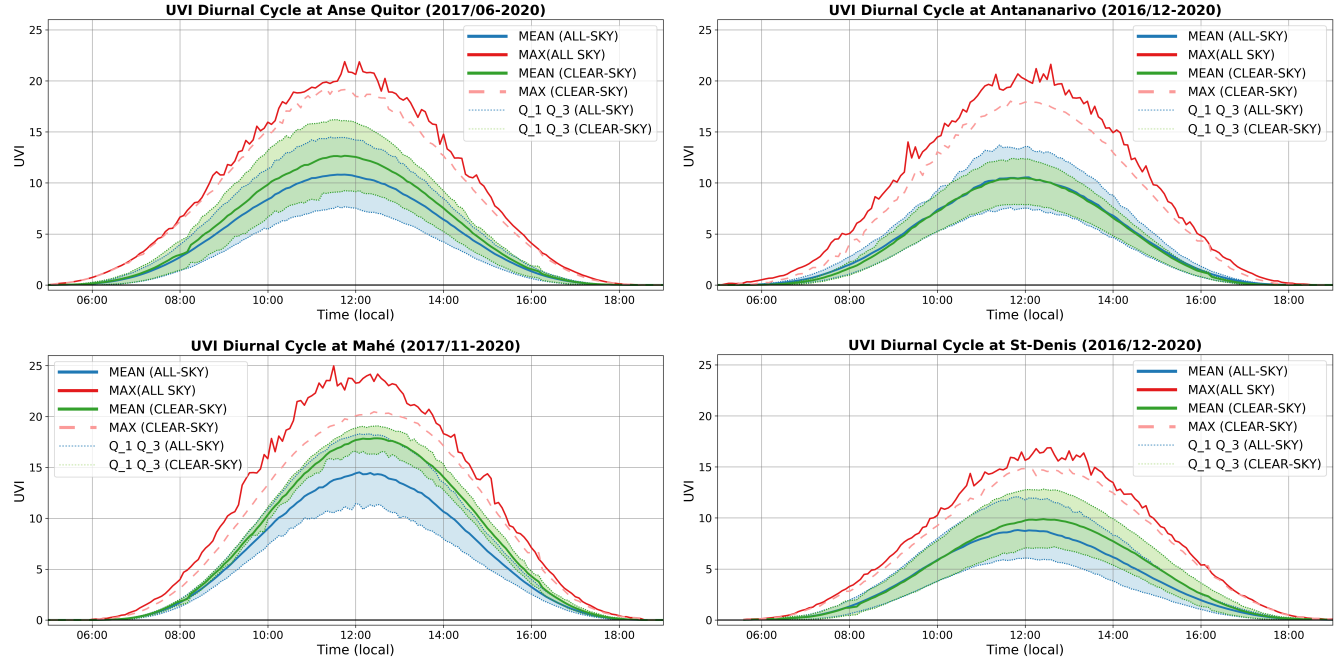

Figure 5. Diurnal Cycle of UVI at ST-DENIS.

In all-sky conditions: Mean UVI in blue, Max UVI in red, First and Third Quartile delimit the blue shaded area. In clear-sky conditions: Mean UVI in green, Max UVI in dashed-red, First and Third Quartile delimit the green shaded area.

https://doi.org/10.5194/essd-2021-55
Preprint. Discussion started: 3 March 2021

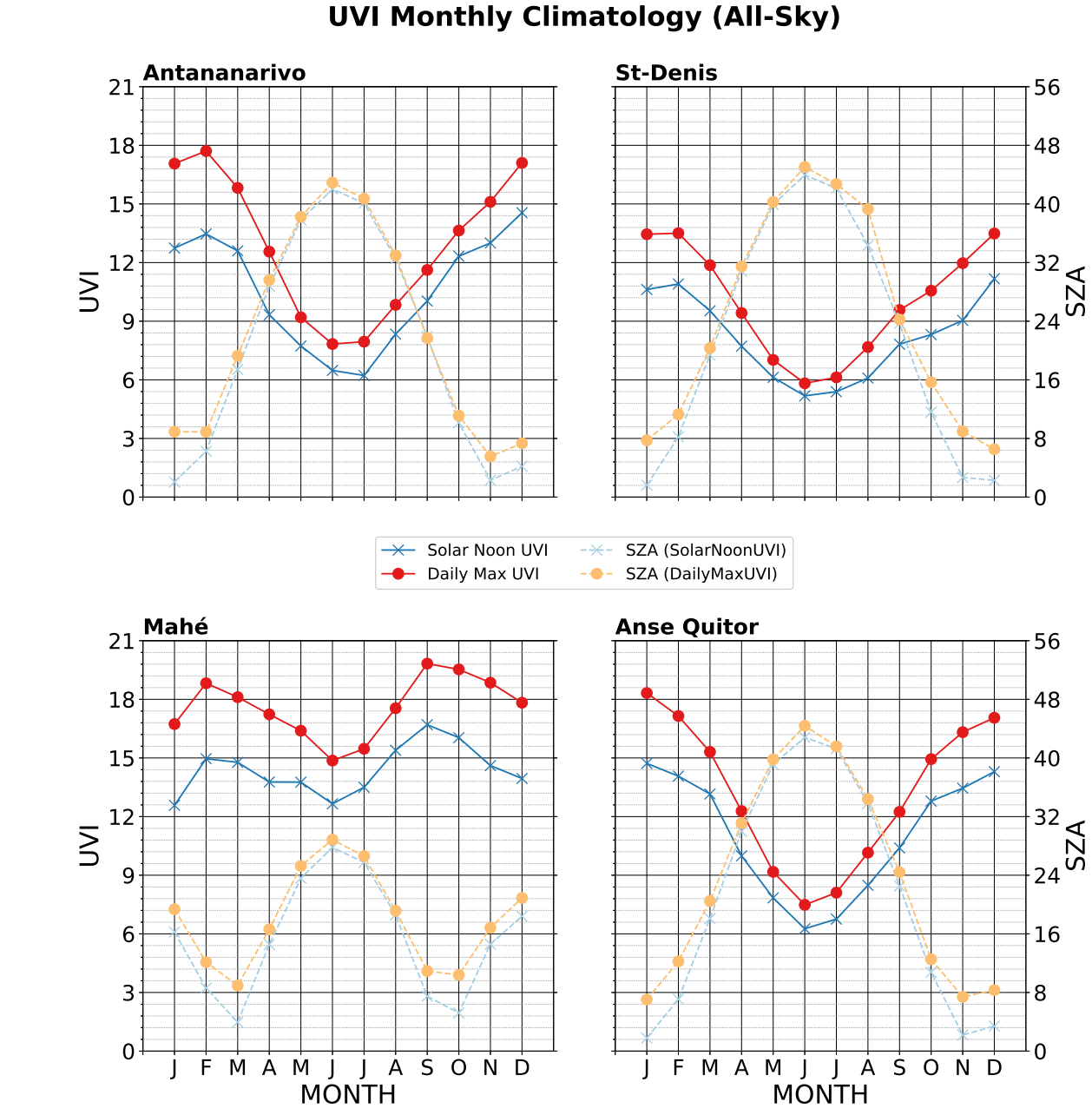

Figure 6. UVI Monthly Climatology in all-sky conditions for the four stations of Antananarivo, St-Denis, Mahé and Anse Quitor. The monthly climatology of the daily max UVI is represented by the red line with filled circles marker. The corresponding SZA is represented by the dotted orange line.

The monthly climatology of the UVI at solar noon is represented by the blue line with blue cross. The corresponding SZA is represented by the blue dashed line.

https://doi.org/10.5194/essd-2021-55
Preprint. Discussion started: 3 March 2021

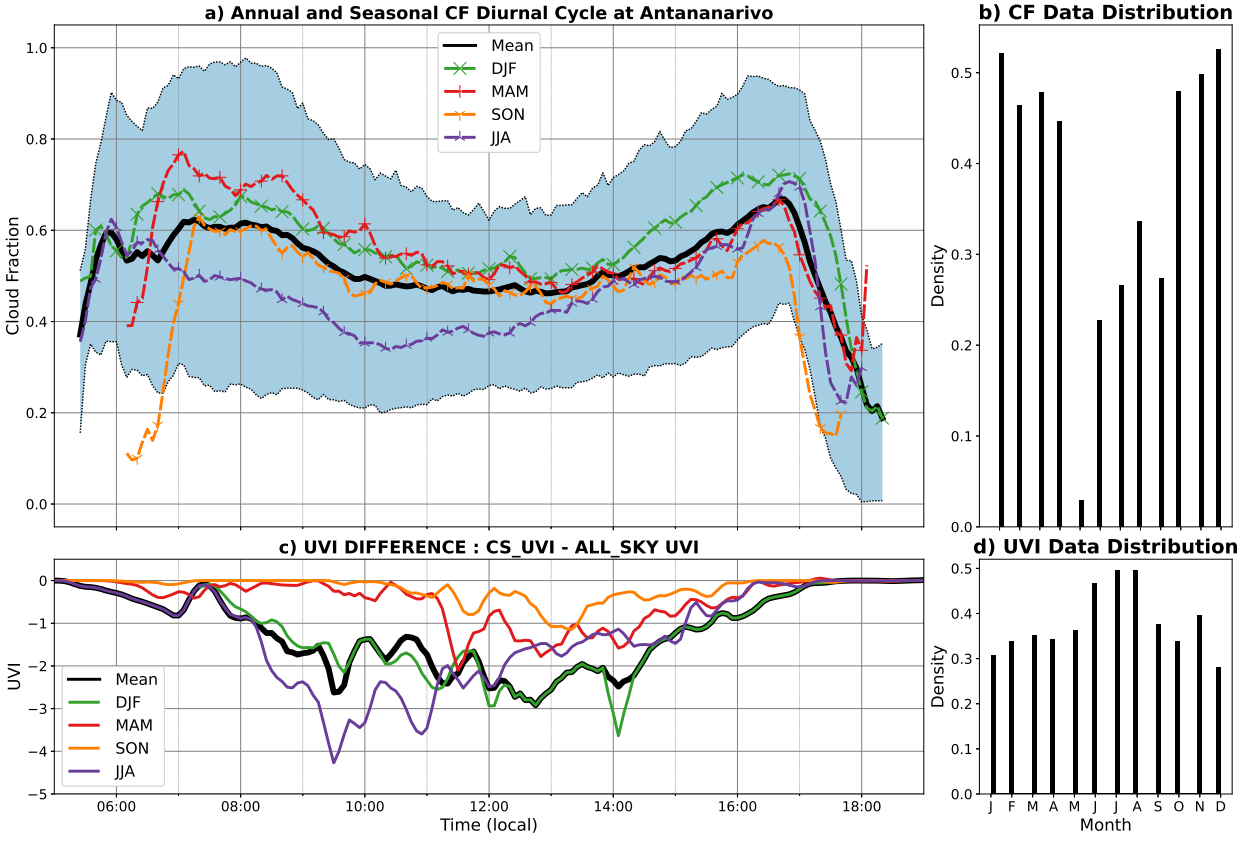

Figure 7. a) and b) Diurnal Cycle of CF at ANTANANARIVO. Annual Mean CF in black, first and third Quartiles delimit the blue shaded area. Seasonal Mean in green (DJF), red (MAM), orange (SON) and purple (JJA).

c) and d) Diurnal Cycle of the difference between maxima of UVI in clear-sky conditions and in all-sky conditions at ANTANANARIVO. Annual Mean UVI differences in black. Seasonal Mean UVI differences in green (DJF), red (MAM), orange (SON) and purple (JJA)

https://doi.org/10.5194/essd-2021-55
Preprint. Discussion started: 3 March 2021

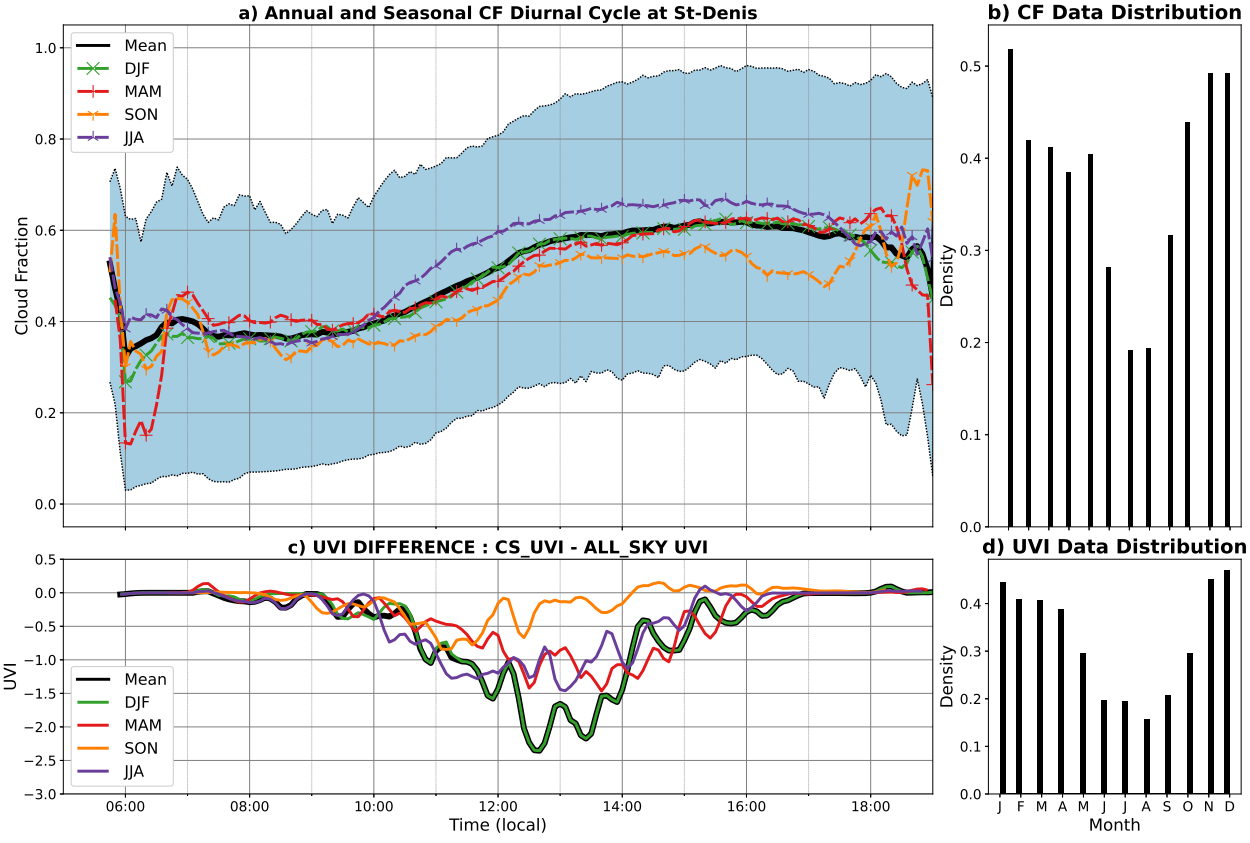

Figure 8. a) and b) Diurnal Cycle of CF at ST-DENIS. Annual Mean CF in black, first and third quartiles delimit the blue shaded area. Seasonal Mean in green (DJF), red (MAM), orange (SON) and purple (JJA).

c) and d) Diurnal Cycle of the difference between maxima of UVI in clear-sky conditions and in all-sky conditions at ST-DENIS. Annual Mean UVI differences in black. Seasonal Mean UVI differences in green (DJF), red (MAM), orange (SON) and purple (JJA)

https://doi.org/10.5194/essd-2021-55
Preprint. Discussion started: 3 March 2021

Open Access Earth System Science Data Discussions

Station	Location	Coordinates	Altitude asl	Instrument	Data since	Frequency	UTC+
Saint-Denis	Reunion	20.902°S, 55.485°E	82m	BENTHAM DTMc 300	2009/01	15 min	+4
				Radiometer Kipp Zonen UVS-E-T 15-0124	2016/12	5 min	
				All Sky Camera	2016/10	1 min	
Maido	Reunion	21.079°S, 55.383°E	2200m	Radiometer Kipp Zonen SUV-E 18-0020	2020/02	1 min	+4
Anse Quitor	Rodrigues	19.758°S, 63.368°E	32m	Radiometer Kipp Zonen UVS-E-T 16-0158	2017/06	1 min	+4
				All Sky Camera	2019/09	1min	
Mahé	Seychelles	4.679 °S, 55.531 °E	15m	Radiometer Kipp Zonen UVS-E-T 17-0207	2017/11	5 min	+4
Antananarivo	Madagascar	18.916°S, 47.565°E	1370m	Radiometer Kipp Zonen UVS-E-T 16-0159	2016/12	5 min	+3
				All Sky Camera	2019/04	1 min	
Diego Suarez	Madagascar	12.279°S, 49.287°E	35m	Radiometer Kipp Zonen SUV-E 18-0028	2019/11	1 min	+3
Fort Dauphin	Madagascar	25.028°S, 46.995°E	10m	Radiometer Kipp Zonen SUV-E 18-0030	2020/01	1 min	+3
				All Sky Camera	2020/01	1 min	
Moroni	Comores	11.708°S 43.247°E	12m	Radiometer Kipp Zonen SUV-E 18-0027	2019/12	1 min	+3
				All Sky Camera	2019/12	1 min	
Juan de Nova	France	17.054°S, 42.711°E	10m	Radiometer Kipp Zonen SUV-E 18-0029	2019/04	1 min	+3

Table 1. Stations of the UV-Indien Project

https://doi.org/10.5194/essd-2021-55
Preprint. Discussion started: 3 March 2021

Open Access Earth System Science Data Discussions

Dataset	Platform	Type	Resolution	Field used for computation/calibration		References
				Ozone field used	Aerosol field used	
BENTHAM	Ground-Based	Spectrometer	dt = 15min	None	None	Brogniez et al. (2016)
Radiometer K&Z (UVI-RADIO)	Ground-Based	Radiometer	dt = 1 or 5 min	SAOZ or OMI	None	Cadet et al. (2020)
OMUVBG	Satellite	Spectrometer (Measurement at 360nm then Table Look-Up)	Daily (Overpass/Solar Noon) 0.25 x 0.25 deg.	OMI	OMI Krotkov et al. (1998) Herman et al. (2009)	Tanskanen et al. (2006) Arola et al. (2009) Levelt et al. (2006)
TROPOMI	Satellite	Spectrometer (Measurement at 354nm then Table Look-Up)	Daily (Overpass/Solar Noon) 5.6 x 3.7 km	TROPOMI L2 total ozone column product Garane et al. (2019).	Aerosol Climatology Kinne et al. (2013)	Lindfors et al. (2018) Lakkala et al. (2020)
GOME	Satellite	Spectrometer	Daily (local solar noon) 0.5 x 0.5 deg.	GOME-2A TOZ	MODIS Level 3	Kujanpää and Kalakoski (2015)
CAMS	Model	Modelling	dt = 6 hours 40km (after 2016-06-21) 80 km (before 2016-06-21)	Modelled	Modelled	Bozzo A. (2015)
TEMIS	Model	Modelling	Daily (local solar noon) 0.5 x 0.5 deg.	SCIAMACHY GOME-2A MSR	No direct correction	Zempila et al. (2017)

Table 2. Satellites, Model and ground-based data used in this study.

Radiometer	Current Calibration	Next Calibration Date	Current Location
UVS-E-T 15-0124	Bentham	05/2021	Saint-Denis
UVS-E-T 16-0159	Manufacturer	06/2020	Antananarivo
UVS-E-T 16-0158	Manufacturer	06/2020	Anse Quitor
UVS-E-T 17-0207	Manufacturer	06/2020	Mahé
SUV-E 18-0020	Bentham	03/2022	Maido
SUV-E 18-0028	Bentham	03/2022	Diego Suarez
SUV-E 18-0030	Bentham	03/2022	Fort Dauphin
SUV-E 18-0027	Bentham	03/2022	Moroni
SUV-E 18-0029	Bentham	03/2022	Juan de Nova

Table 3. Radiometers of the UV-Indien Network.

https://doi.org/10.5194/essd-2021-55
Preprint. Discussion started: 3 March 2021

Open Access Earth System Science Data Discussions

	SAT/MODEL Comparison Against CS-UVI-BENTHAM (ALL-SKY-UVI BENTHAM) at ST-DENIS					
STATS	**UVI-CAMS**	**UVI-OMUVBG**	**UVI-TROPOMI**	**UVI-GOME-SN**	**UVI-TEMIS-SN**	**UVI-RADIO**
MEAN-AD	0.47 ± 0.55 (1.09 ± 1.97)	0.09 ± 2.36 (0.34 ± 2.54)	-0.25 ± 0.73 (0.60 ± 1.83)	-0.01 ± 0.68 (1.23 ± 2.86)	0.40 ± 0.62 (2.31 ± 3.26)	-0.03 ± 0.39 (0.02 ± 0.65)
MEAN-RD	12.33 ± 12.27 (48.36 ± 105.87)	8.54 ± 53.93 (23.95 ± 82.00)	-3.13 ± 10.09 (30.85 ± 70.85)	0.78 ± 8.66 (40.31 ± 123.55)	3.61 ± 7.12 (59.73 ± 164.38)	-2.95 ± 12.16 (0.32 ± 23.77)
MEDIAN-AD	0.21 (0.50)	-0.15 (-0.06)	-0.16 (0.21)	-0.01 (0.30)	0.27 (0.96)	-0.02 (-0.00)
MEDIAN-RD	11.32 (14.20)	-3.98 (-1.03)	-2.52 (3.98)	-0.07 (3.48)	3.27 (10.15)	-1.17 (-0.14)
NDATA	1038 (3069)	145 (408)	254 (1555)	120 (750)	142 (919)	34665 (93300)

Table 4. Mean and Median Absolute and Relative Differences between CS-UVI Sat/Model Measurements and CS-UVI-BENTHAM and at ST-DENIS. Mean and Median Absolute and Relative Differences between ALL-SKY-UVI Sat/Model Measurements and ALL-SKY-UVI-BENTHAM and at ST-DENIS in parentheses

https://doi.org/10.5194/essd-2021-55
Preprint. Discussion started: 3 March 2021

Open Access Earth System Science Data Discussions

Appendix A

A1

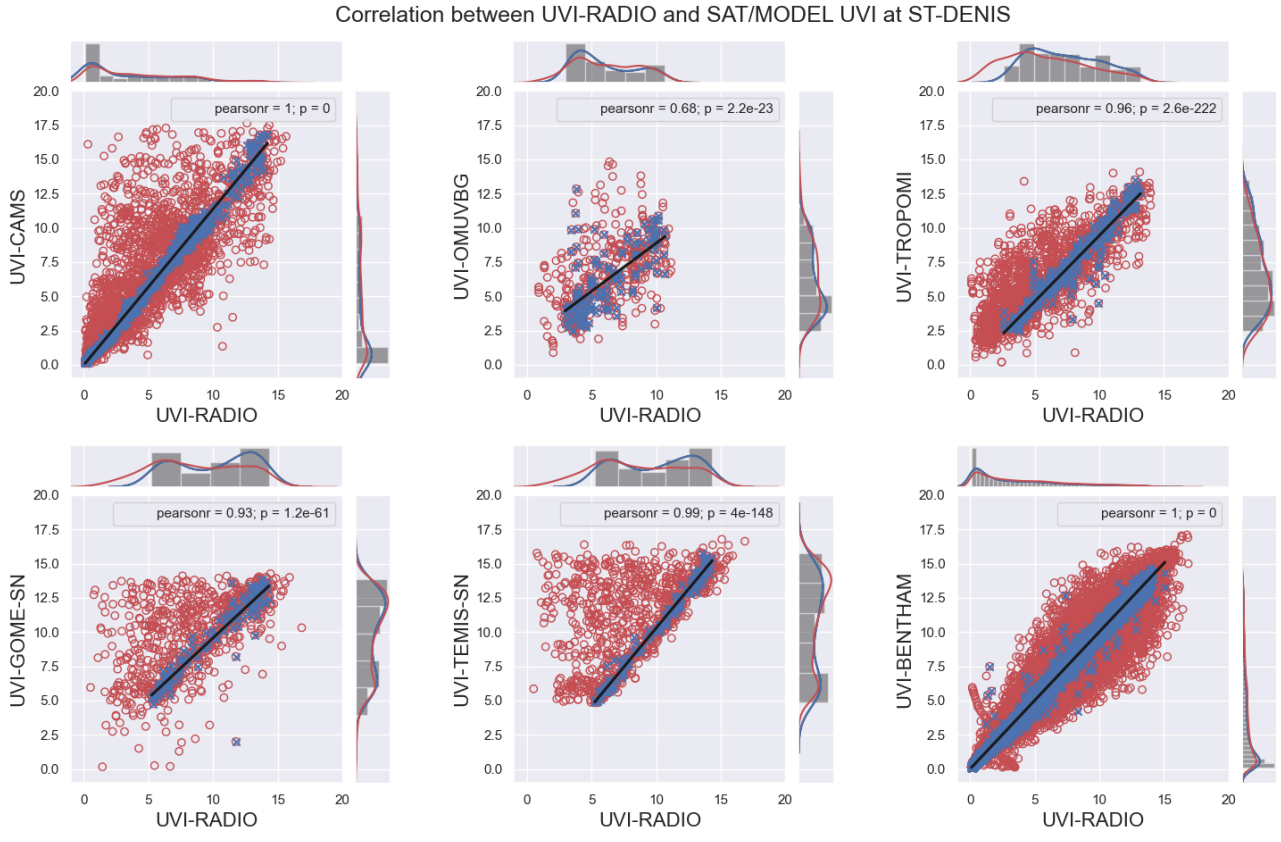

Figure A1. Correlation between UVI-RADIO and Sat/Model Estimates at ST-DENIS

https://doi.org/10.5194/essd-2021-55
Preprint. Discussion started: 3 March 2021

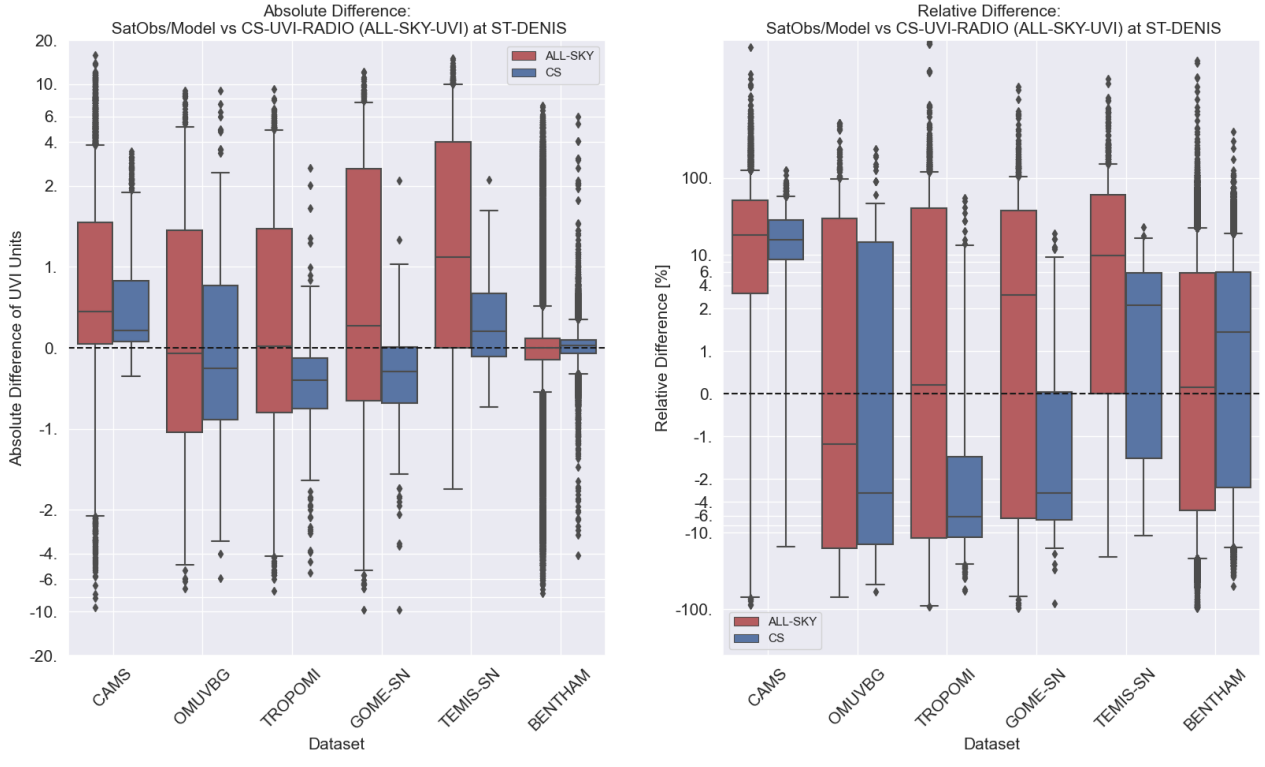

Figure A2. Boxplot of differences between UVI-RADIO and Sat/Model Estimates at ST-DENIS.

https://doi.org/10.5194/essd-2021-55
Preprint. Discussion started: 3 March 2021

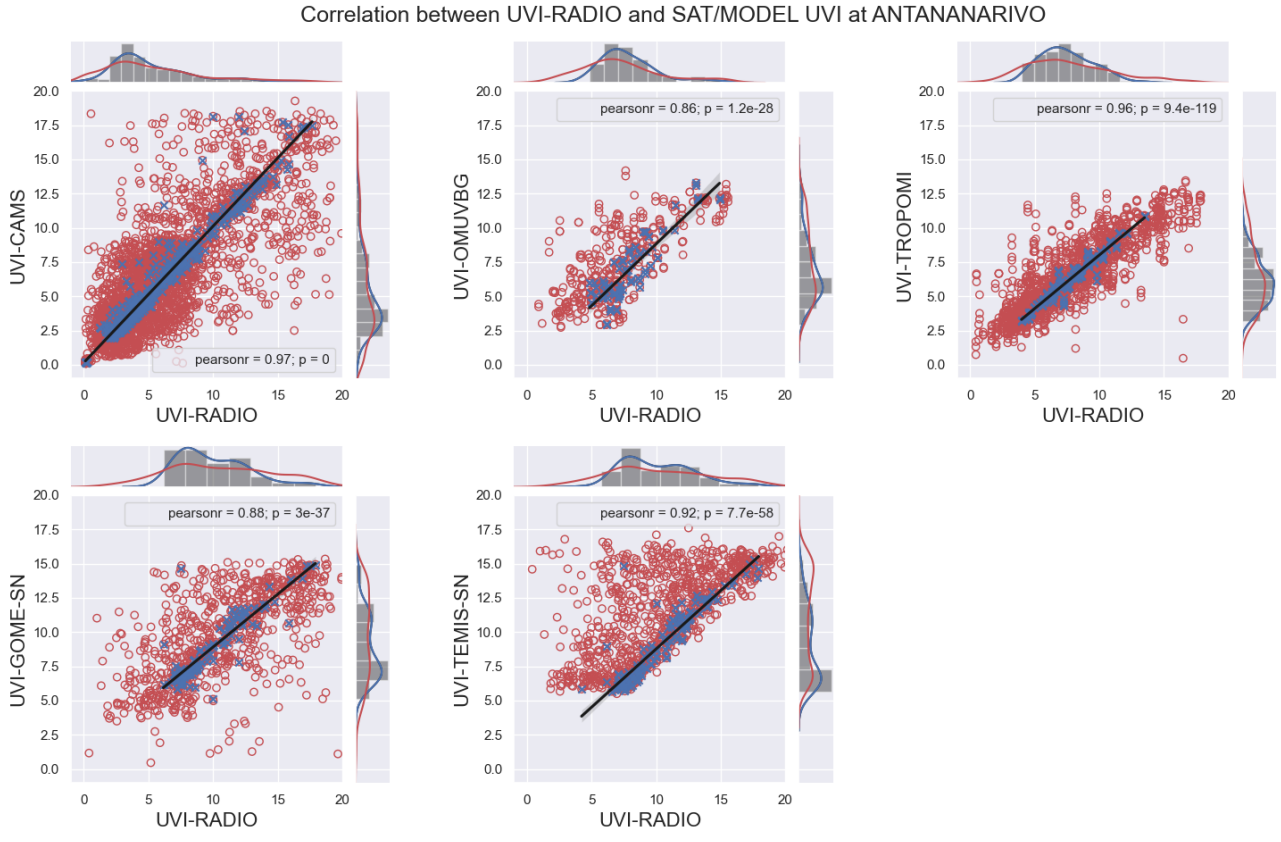

Figure A3. Correlation between UVI-RADIO and Sat/Model Estimates at ANTANANARIVO.

https://doi.org/10.5194/essd-2021-55
Preprint. Discussion started: 3 March 2021

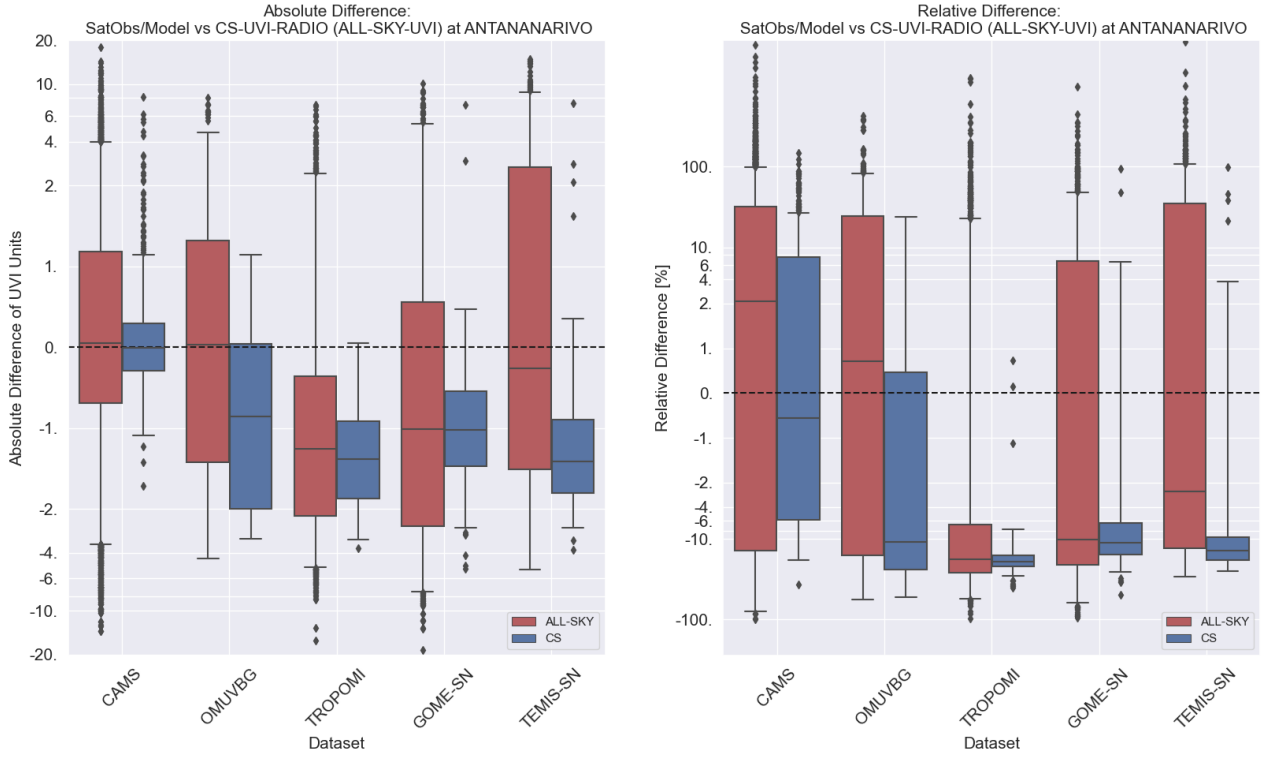

Figure A4. Boxplot of differences between UVI-RADIO and Sat/Model Estimates at ANTANANARIVO.

https://doi.org/10.5194/essd-2021-55
Preprint. Discussion started: 3 March 2021

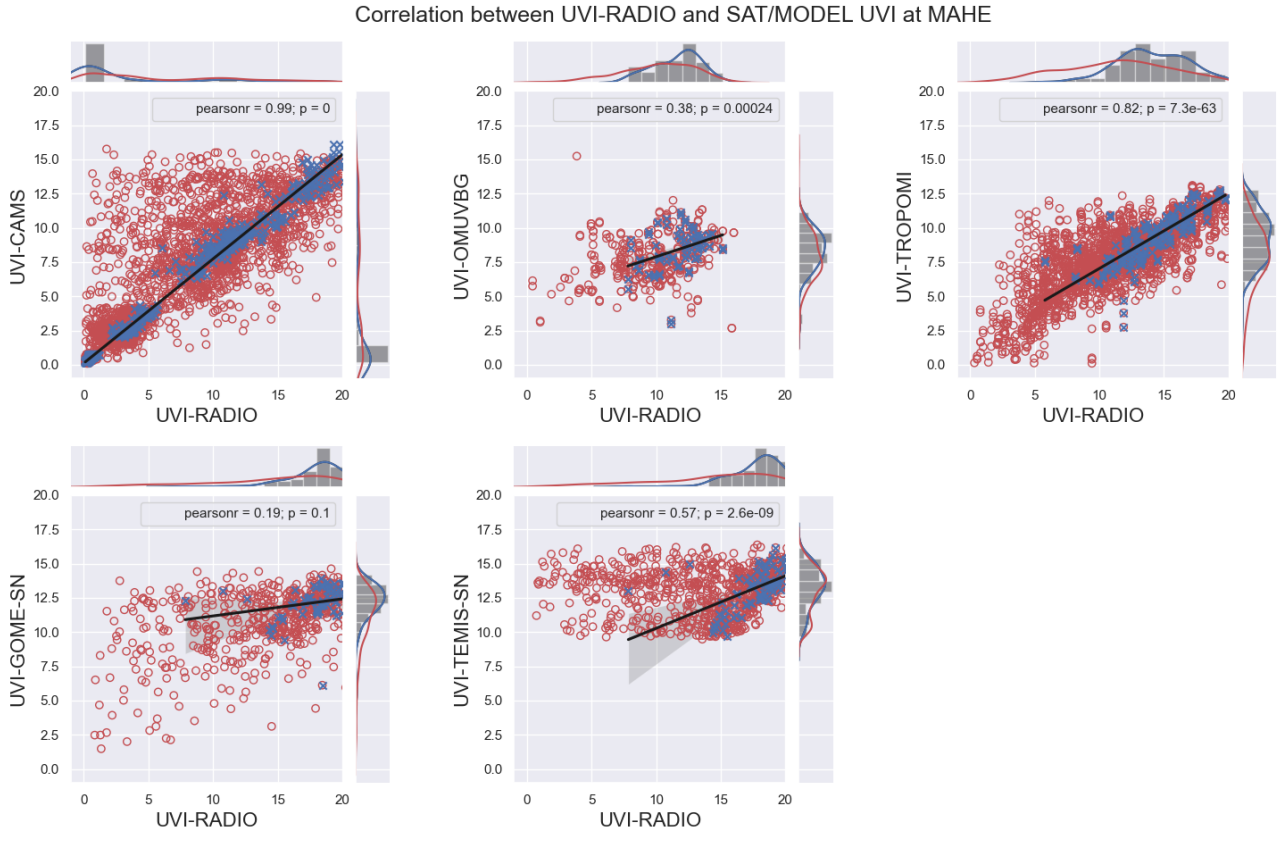

Figure A5. Correlation between UVI-RADIO and Sat/Model Estimates at MAHE.

https://doi.org/10.5194/essd-2021-55
Preprint. Discussion started: 3 March 2021

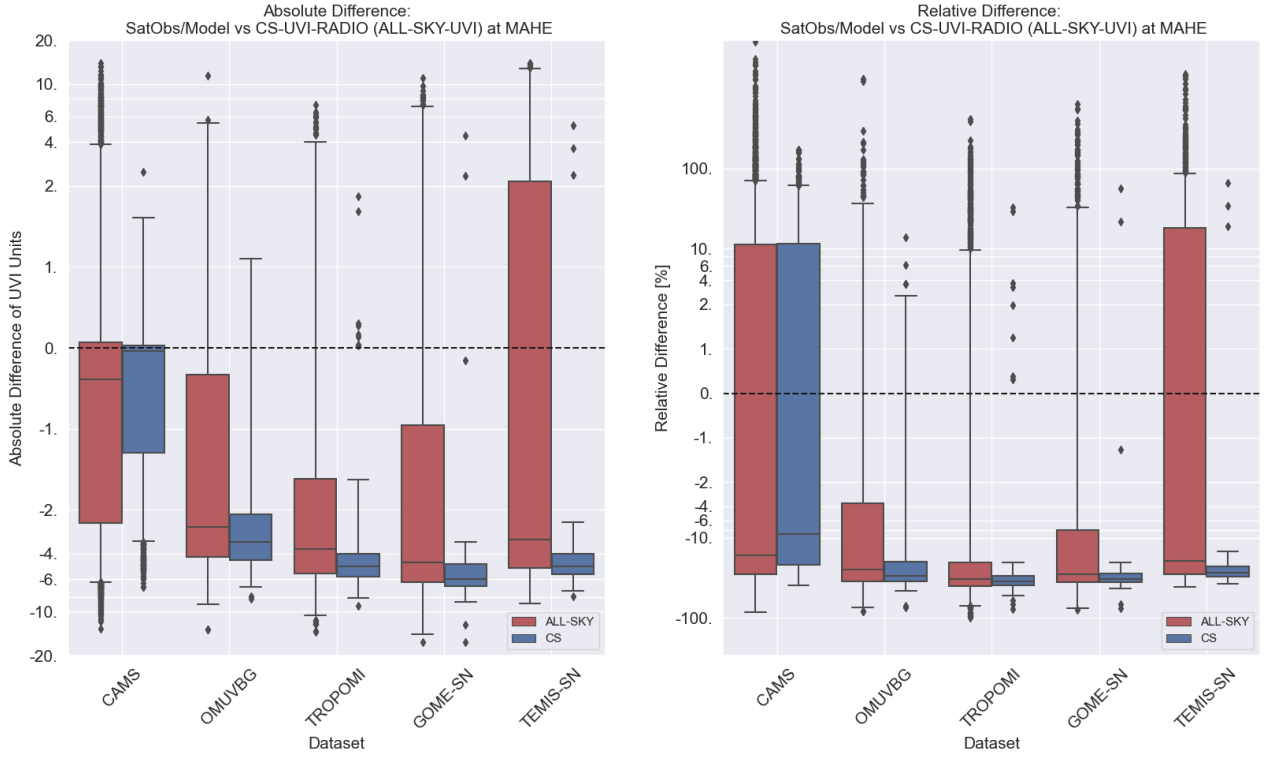

Figure A6. Boxplot of differences between UVI-RADIO and Sat/Model Estimates at MAHE.

https://doi.org/10.5194/essd-2021-55
Preprint. Discussion started: 3 March 2021

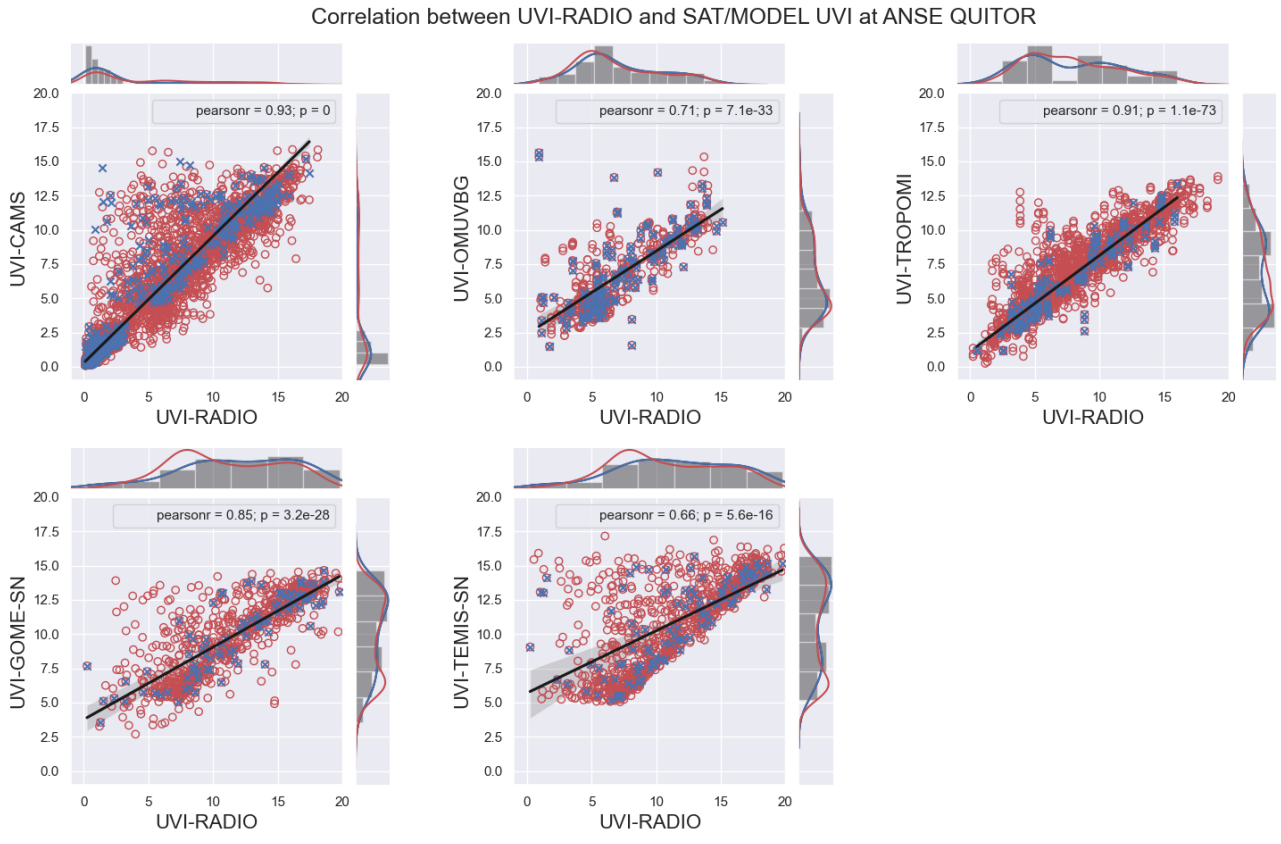

Figure A7. Correlation between UVI-RADIO and Sat/Model Estimates at ANSE QUITOR.

https://doi.org/10.5194/essd-2021-55
Preprint. Discussion started: 3 March 2021

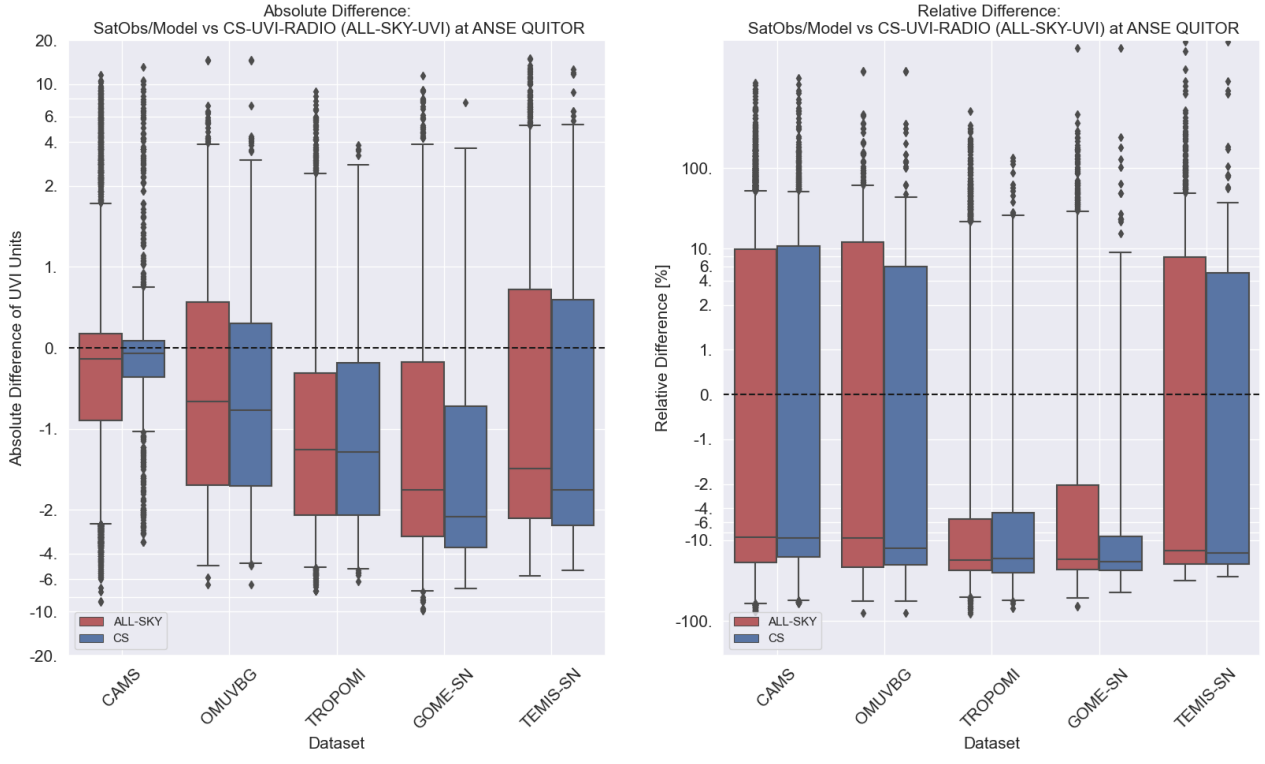

Figure A8. Boxplot of differences between UVI-RADIO and Sat/Model Estimates at ANSE QUITOR.

https://doi.org/10.5194/essd-2021-55
Preprint. Discussion started: 3 March 2021

Open Access Earth System Science Data Discussions

	Comparison of SAT/MODEL with CS-UVI-RADIO (ALL-SKY-UVI RADIO) at ST-DENIS					
STATS	**UVI-CAMS**	**UVI-OMUVBG**	**UVI-TROPOMI**	**UVI-GOME-SN**	**UVI-TEMIS-SN**	**UVI-BENTHAM**
MEAN-AD	0.51 ± 0.63 (1.08 ± 2.19)	0.07 ± 1.89 (0.38 ± 2.47)	-0.46 ± 0.75 (0.39 ± 1.95)	-0.43 ± 1.10 (1.09 ± 2.92)	0.29 ± 0.58 (2.39 ± 3.24)	0.02 ± 0.22 (-0.02 ± 0.64)
MEAN-RD	20.12 ± 18.11 (51.13 ± 140.84)	6.22 ± 41.58 (21.24 ± 77.44)	-6.45 ± 10.87 (46.13 ± 290.98)	-3.53 ± 9.84 (34.69 ± 112.84)	1.80 ± 6.12 (57.14 ± 141.93)	4.17 ± 13.00 (1.97 ± 24.99)
MEDIAN-AD	0.21 (0.45)	-0.25 (-0.07)	-0.40 (0.02)	-0.29 (0.27)	0.20 (1.12)	0.03 (0.00)
MEDIAN-RD	15.80 (18.01)	-3.03 (-1.19)	-6.24 (0.21)	-3.08 (3.01)	2.22 (9.86)	1.45 (0.14)
NDATA	1279 (4087)	160 (467)	387 (1988)	141 (893)	164 (1069)	29488 (92864)

Table A1. Mean and Median Absolute and Relative Differences between CS-UVI Sat/Model Measurements and CS-UVI-RADIO and at ST-DENIS. Mean and Median Absolute and Relative Differences between ALL-SKY-UVI Sat/Model Measurements and ALL-SKY-UVI-RADIO and at ST-DENIS in parentheses

	Comparison of SAT/MODEL with CS-UVI-RADIO (ALL-SKY-UVI RADIO) at ANTANANARIVO				
STATS	**UVI-CAMS**	**UVI-OMUVBG**	**UVI-TROPOMI**	**UVI-GOME-SN**	**UVI-TEMIS-SN**
MEAN-AD	0.14 ± 0.84 (0.18 ± 2.64)	-0.96 ± 1.16 (0.10 ± 2.24)	-1.43 ± 0.61 (-1.35 ± 1.91)	-1.10 ± 1.27 (-1.00 ± 3.23)	-1.25 ± 1.11 (0.77 ± 3.20)
MEAN-RD	4.03 ± 18.53 (21.40 ± 113.35)	-12.16 ± 15.84 (13.53 ± 58.09)	-18.94 ± 5.65 (-8.93 ± 61.87)	-10.09 ± 13.80 (1.39 ± 58.78)	-11.96 ± 13.22 (26.44 ± 139.83)
MEDIAN-AD	-0.01 (0.05)	-0.86 (0.04)	-1.38 (-1.26)	-1.02 (-1.01)	-1.41 (-0.26)
MEDIAN-RD	-0.55 (2.13)	-10.98 (0.71)	-19.11 (-18.02)	-11.11 (-10.10)	-14.13 (-2.59)
NDATA	564 (3337)	92 (427)	203 (1796)	111 (816)	142 (992)

Table A2. Mean and Median Absolute and Relative Differences between CS-UVI Sat/Model Measurements and CS-UVI-RADIO and at ANTANANARIVO. Mean and Median Absolute and Relative Differences between ALL-SKY-UVI Sat/Model Measurements and ALL-SKY-UVI-RADIO and at ANTANANARIVO in parentheses

https://doi.org/10.5194/essd-2021-55
Preprint. Discussion started: 3 March 2021

Open Access Earth System Science Data Discussions

	Comparison of SAT/MODEL with CS-UVI-RADIO (ALL-SKY-UVI RADIO) at MAHE				
STATS	**UVI-CAMS**	**UVI-OMUVBG**	**UVI-TROPOMI**	**UVI-GOME-SN**	**UVI-TEMIS-SN**
MEAN-AD	-0.82 ± 1.44 (-0.93 ± 2.94)	-3.22 ± 1.83 (-2.16 ± 2.95)	-4.80 ± 1.60 (-3.48 ± 2.88)	-5.75 ± 2.51 (-3.41 ± 4.29)	-4.52 ± 1.82 (-1.22 ± 4.99)
MEAN-RD	-1.23 ± 28.57 (11.52 ± 140.58)	-26.62 ± 14.30 (-6.28 ± 101.10)	-33.43 ± 10.43 (-24.98 ± 31.94)	-30.65 ± 14.98 (-6.92 ± 69.82)	-24.46 ± 13.08 (23.62 ± 144.59)
MEDIAN-AD	-0.04 (-0.39)	-3.31 (-2.63)	-4.88 (-3.73)	-5.99 (-4.59)	-4.91 (-3.19)
MEDIAN-RD	-8.91 (-16.41)	-29.49 (-24.85)	-34.58 (-32.70)	-32.25 (-28.55)	-27.11 (-19.15)
NDATA	1133 (3525)	89 (392)	253 (2132)	72 (635)	94 (881)

Table A3. Mean and Median Absolute and Relative Differences between CS-UVI Sat/Model Measurements and CS-UVI-RADIO and at MAHE. Mean and Median Absolute and Relative Differences between ALL-SKY-UVI Sat/Model Measurements and ALL-SKY-UVI-RADIO and at MAHE in parentheses

	Comparison of SAT/MODEL with CS-UVI-RADIO (ALL-SKY-UVI RADIO) at ANSE QUITOR				
STATS	**UVI-CAMS**	**UVI-OMUVBG**	**UVI-TROPOMI**	**UVI-GOME-SN**	**UVI-TEMIS-SN**
MEAN-AD	0.06 ± 1.49 (-0.20 ± 1.82)	-0.43 ± 2.36 (-0.36 ± 2.19)	-1.28 ± 1.69 (-1.19 ± 1.80)	-1.88 ± 2.58 (-1.42 ± 2.71)	-0.55 ± 3.34 (-0.39 ± 3.06)
MEAN-RD	12.02 ± 91.52 (6.85 ± 69.67)	17.36 ± 163.36 (12.16 ± 114.22)	-10.93 ± 26.62 (-8.71 ± 35.26)	26.16 ± 319.83 (0.12 ± 121.81)	56.15 ± 376.30 (18.21 ± 179.43)
MEDIAN-AD	-0.06 (-0.14)	-0.77 (-0.66)	-1.28 (-1.25)	-2.23 (-1.75)	-1.75 (-1.49)
MEDIAN-RD	-9.28 (-9.20)	-12.56 (-9.45)	-16.65 (-17.68)	-18.47 (-17.10)	-14.51 (-13.31)
NDATA	996 (3956)	204 (516)	189 (2114)	95 (752)	115 (964)

Table A4. Mean and Median Absolute and Relative Differences between CS-UVI Sat/Model Measurements and CS-UVI-RADIO and at ANSE QUITOR. Mean and Median Absolute and Relative Differences between ALL-SKY-UVI Sat/Model Measurements and ALL-SKY-UVI-RADIO and at ANSE QUITOR in parentheses